Supporting Information

Carbodiimides as Catalysts for the Reduction of CO_2 with Boranes

Alberto Ramos,*[a] Antonio Antiñolo,*[a] Fernando Carrillo-Hermosilla,[a] Rafael Fernández-Galán,[a] Antonio Rodríguez-Diéguez,[b] Daniel García-Vivó[c]

[a] *Departamento de Química Inorgánica, Orgánica y Bioquímica, Facultad de Ciencias y Tecnologías Químicas, Universidad de Castilla-La Mancha, Campus Universitario, E-13071 Ciudad Real, Spain.*

[b] *Departamento de Química Inorgánica, Facultad de Ciencias, Universidad de Granada, Avenida de la Fuente Nueva S/N, 18071 Granada, Spain.*

[c] *Departamento de Química Orgánica e Inorgánica/IUQOEM, Universidad de Oviedo, E-33071 Oviedo, Spain.*

*Email: Alberto.Ramos@uclm.es

CONTENTS

General remarks. All manipulations were carried out under dry nitrogen (or CO_2) using standard Schlenk and glovebox techniques. Solvents were distilled from appropriate drying agents and stored under N_2 in Schlenk tubes equipped with J. Young-type Teflon stoppers and containing activated molecular sieves (4 Å). Microanalyses were carried out with a LECO CHNS-932 analyser. NMR spectra were recorded on Bruker 400 and 500 spectrometers in C_6D_6 at 298 K unless otherwise stated, using standard TOPSPIN 4.0 software. ^{1}H NMR and ^{13}C{^{1}H} NMR chemical shifts are referenced to residual protons or carbons in deuterated solvent. Chemical shifts (δ) are given in ppm and coupling constants (J) in Hz. All reagents were purchased from the usual commercial suppliers.

Preparation of CH(N^{i}Pr)$_2$BC$_8$H$_{14}$ (1). To a solution of 9-borabicylo-[3:3:1]-borane (H-BBN or H-BC$_8$H$_{14}$, 366 mg, 3.00 mmol) in toluene (6 mL), *N*,*N*′-diisopropylcarbodiimide (DIC, 465 μL, 3.00 mmol) was added. The solution was stirred for 2h at 60 ºC. Then, the solvent was removed under vacuum to give compound **1** as a colourless oily liquid which solidified upon storing at –20 ºC to become a white solid after pulverisation (620 mg, 83%). Anal. calcd for $C_{15}H_{29}BN_2$: C, 72.58; H, 11.78; N, 11.29. Found: C, 72.65; H, 11.46; N, 11.07. ^{1}H NMR (500 MHz): δ 8.24 (s, 1H, *H*-C=N), 4.88, 3.25 (2 x br, 2 x 1H, 2 x C*H*-^{i}Pr), 2.0 – 1.3 (m, 14H, BC$_8$*H$_{14}$*), 1.30 (br, 12H, 2 x C*H$_3$*-^{i}Pr). ^{13}C{^{1}H} NMR (101 MHz): δ 150.6 (s, H-*C*=N) , 57.6, 46.9 (2 x s, 2 x *C*H-^{i}Pr), 33.6 (s, *C*H$_2$-BC$_8$H$_{14}$, 4C), 25.4 (br, *C*H-BC$_8$H$_{14}$, 2C), 23.5 (s, *C*H$_2$-BC$_8$H$_{14}$, 2C), 22.2 (br, *C*H$_3$-^{i}Pr). ^{11}B NMR (128 MHz): δ 55.8 (br, $\Delta\nu_{1/2}$ *ca*. 280 Hz, B).

Preparation of CH(N^{i}Pr)$_2$(C$_8$H$_{14}$B-H-BC$_8$H$_{14}$) (2). Method A: Solutions containing **2** as the major species were prepared in an NMR scale by adding H-BC$_8$H$_{14}$, (15 mg, 0.12 mmol) to a solution of **1** (25 mg, 0.10 mmol) in C_6D_6. A temperature-dependent equilibrium is established, and a ratio **2**:**1** of ca. 91:9 is reached after 24 h at 25 ºC (^{1}H NMR), which changes to 61:39 upon heating at 60 ºC (see Fig S3). Method B: Alternatively, compound **2** can be prepared from a solution of DIC (155 μL, 1.00 mmol) in toluene (6 mL) by adding H-BC$_8$H$_{14}$ (270 mg, 2.21 mmol) and stirring for 2 h at 60 ºC. After removing the solvent under vacuum, the white solid obtained was dissolved in the minimum amount of toluene (2 mL), which was layered with pentane (4 mL) and kept at –20 ºC to yield crystals of **2**. Then, the solvent was decanted and the crystals were washed with pentane (2 x 2 mL) and dried under vacuum to yield compound **2** as a white crystalline powder (65 mg, 18%). Crystals of **2** suitable for an X-ray diffractometric analysis were grown from a concentrated solution in pentane at –20 ºC. Anal. calcd for

$C_{23}H_{44}B_2N_2$: C, 74.61; H, 11.98; N, 7.57. Found: C, 74.60; H, 11.49; N, 7.39. ^{1}H NMR (500 MHz): δ 7.24 (s, 1H, *H*-C=N), 3.95 (sept, J = 6.7 Hz, 2H, C*H*-^{i}Pr), 2.5 – 1.6 (m, 24H, C*H*$_2$-BC_8H_{14}), 1.31 (br, 4H, C*H*-BC_8H_{14}), 0.94 (d, J = 6.7 Hz, 6H, C*H*$_3$-^{i}Pr), 0.16 (br, 1H, B-*H*-B). ^{13}C{^{1}H} NMR (101 MHz): δ 153.5 (s, H-*C*=N), 48.8 (s, *C*H-^{i}Pr), 34.5, 32.8, 25.5, 24.4 (4 x br, 4 x *C*H$_2$-BC_8H_{14}), 24.0 (br, *C*H-BC_8H_{14}) 23.4 (s, *C*H$_3$-^{i}Pr). ^{11}B NMR (128 MHz): δ 15.6 (br, $\Delta\nu_{1/2}$ *ca*. 280 Hz, 2B).

Preparation of CH(N^{i}Pr)$_2$(CO$_2$)BC$_8$H$_{14}$ (3). A solution of compound **1** (150 mg, 0.60 mmol) in toluene (4 mL) was subjected to a freeze-pump-thaw cycle and was refilled with CO_2 (1 atm) after reaching room temperature again. After 5 min stirring at 25 ºC, a white precipitate (compound **3**) was already observed. The suspension was further stirred for 15 h to allow full conversion. At this point, pentane (5 mL) was added and the suspension was filtered. The solid remaining on the frit was washed with more pentane (3 x 5 mL) and dried under vacuum to give compound **3** as a white powder (125 mg, 71%). Crystals of **3** suitable for an X-ray diffraction analysis were grown upon exposure of a solution of **1** in C_6D_6 to a CO_2 atmosphere at 25 ºC. Anal. calcd for $C_{16}H_{29}BN_2O_2$: C, 65.76; H, 10.00; N, 9.59. Found: C, 65.81; H, 9.66; N, 9.46. ^{1}H NMR (400 MHz, CD_2Cl_2) δ 7.60 (s, 1H, *H*-C=N), 4.60 (sept, J = 6.9 Hz, 1H, C*H*-^{i}Pr), 4.37 (sept, J = 6.6 Hz, 1H, C*H*-^{i}Pr), 2.1 – 1.4 (m, 12H, C*H*$_2$-BC_8H_{14}), 1.35 (d, J = 6.6 Hz, 6H, C*H*$_3$-^{i}Pr), 1.31 (d, J = 6.9 Hz, 6H, C*H*$_3$-^{i}Pr), 0.77 (br, 2H, C*H*-BC_8H_{14}). ^{13}C{^{1}H} NMR (101 MHz, CD_2Cl_2): δ 151.0 (s, *C*O$_2$), 149.3 (s, H-*C*=N), 52.3, 49.0, (2 x s, 2 x *C*H-^{i}Pr), 32.6, 31.6, (2 x s, 2 x *C*H$_2$-BC_8H_{14}, 2 x 2C), 24.4, 24.0 (2 x s, 2 x *C*H$_2$-BC_8H_{14}, 2 x 1C), 23.6 (br, *C*H-BC_8H_{14}, 2C), 23.2, 21.9 (2 x s, 2 x *C*H$_3$-^{i}Pr). ^{11}B NMR (128 MHz, CD_2Cl_2): δ 5.9 (br, $\Delta\nu_{1/2}$ *ca*. 150 Hz, B).

Preparation of CH(N^{i}Pr)$_2$(CH$_2$O)BC$_8$H$_{14}$ (4). Method A: Excess paraformaldehyde (75 mg, 2.38 mmol) was added to a solution of compound **1** (248 mg, 1.00 mmol) in toluene (5 mL). The suspension was stirred for 2 h at 60 ºC. After this time, it was filtered to eliminate the excess of paraformaldehyde. The solvent was then removed under vacuum and a viscous oil containing **4** was obtained. Then, pentane was added (5 mL), and the solution was stirred for 5 min. The solvent was subsequently removed under vacuum to yield a waxy solid/oil mixture. This process was repeated two more times until compound **4** was obtained as a white powder (235 mg, 84%). Method B: Solutions containing **4** could also be obtained in NMR scale by mixing compound **3** (7 mg, 0.024 mmol) and H-BC_8H_{14} (11 mg, 0.090 mmol) in C_6D_6 (0.6 mL) and heating for 3 days at 60 ºC. After this

time, amidinate derivatives **2**, **3** and **4** were detected by ^{1}H NMR in a ratio ca. 12:5:83, alongside excess H-BC_8H_{14} and $O(BC_8H_{14})_2$ detected by ^{11}B NMR (see Fig S6). Crystals of **4** suitable for an X-ray analysis were grown from a concentrated solution in pentane at –20 ºC. Anal. calcd for $C_{16}H_{31}BN_2O$: C, 69.07; H, 11.23; N, 10.07. Found: C, 68.99; H, 10.84; N, 9.80. ^{1}H NMR (500 MHz) δ 6.88 (s, 1H, *H*-C=N), 4.72 (s, 2H, C*H*$_2$O), 4.24 (sept, J = 6.8 Hz, 1H, C*H*-^{i}Pr), 2.51 (sept, J = 6.8 Hz, 1H, C*H*-^{i}Pr), 2.8 – 2.0 (m, 12H, C*H*$_2$-BC_8H_{14}), 1.17 (br, 2H, C*H*-BC_8H_{14}), 0.94 (d, J = 6.8 Hz, 6H, C*H*$_3$-^{i}Pr), 0.59 (d, J = 6.8 Hz, 6H, C*H*$_3$-^{i}Pr). ^{13}C{^{1}H} NMR (126 MHz) δ 148.2 (s, H-*C*=N), 71.2 (s, H_2*C*-O), 52.3, 49.4 (2 x s, 2 x *C*H-^{i}Pr), 33.0 (br, *C*H_2-BC_8H_{14}), 25.6 (s, *C*H_2-BC_8H_{14}), 24.8 (br, *C*H-BC_8H_{14}), 23.4, 20.9 (2 x s, 2 x *C*H_3-^{i}Pr). ^{11}B NMR (160 MHz): δ 3.0 (br, $\Delta\nu_{1/2}$ *ca*. 105 Hz, B).

Preparation of $CH_2(N^iPr)_2BH(N^iPr)C=N(^iPr)\cdot BH_3$ (5). A solution of $BH_3\cdot SMe_2$ (290 μL, 3.00 mmol) in toluene (2 mL) was added dropwise to another solution of DIC (310 μL, 2.00 mmol) in toluene (2 mL). Heat is immediately released upon addition due to formation of **5**. Then, the mixture was further stirred for 5 min to ensure completion of the reaction. After that, pentane (8 mL) was added and the mixture was stored at –20 ºC to obtain a white precipitate. The solid was collected by filtration, washed with pentane (4 x 5 mL), and dried under vacuum to yield **5** as a white solid (165 mg, 59%). Crystals of **5** suitable for an X-ray diffraction analysis were grown from a concentrated solution of CH_2Cl_2 / pentane (1:4) kept at –20 ºC. Anal. calcd for $C_{14}H_{34}B_2N_4$: C, 60.04; H, 12.24; N, 20.00. Found: C, 59.96; H, 11.82; N, 19.95. ^{1}H NMR (500 MHz) δ 4.60 (sept, J = 6.7 Hz, 1H, C*H*-^{i}Pr), 4.42 (sept, J = 6.8 Hz, 1H, C*H*-^{i}Pr), 4.33 (vbr, 1H, B*H*), 3.63 (sept, J = 6.5 Hz, 1H, C*H*-^{i}Pr), 3.57 (AB, J = 11.5 Hz, 2H, C*H*$_2$N$_2$), 2.77 (sept, J = 6.5 Hz, 1H, C*H*-^{i}Pr), 2.67 (vbr, 3H, B*H*$_3$), 1.62 (d, br, J ≈ 6.5 Hz, 3H, C*H*$_3$-^{i}Pr), 1.52 (d, br, J ≈ 6.5 Hz, 3H, C*H*$_3$-^{i}Pr), 1.15 (br, 3H, C*H*$_3$-^{i}Pr), 1.07 (br, 6H, 2 x C*H*$_3$-^{i}Pr), 0.83 (d, J = 6.6 Hz, 6H, 2 x C*H*$_3$-^{i}Pr), 0.79 (br, 3H, C*H*$_3$-^{i}Pr). ^{13}C{^{1}H} NMR (126 MHz) δ 163.2 (s, *C*=N), 55.6 (s, *C*H_2), 54.4, 51.6, 51.4, 49.8 (4 x s, 4 x *C*H-^{i}Pr), 25.2, 23.6, 23.5, 23.4, 23.0, 22.7, 21.2, 20.8 (8 x s, 8 x br, 8 x *C*H_3-^{i}Pr). ^{11}B NMR (160 MHz): δ 28.0 (br, $\Delta\nu_{1/2}$ *ca*. 370 Hz, *B*H), –19.9 (q, J_{BH} *ca*. 90 Hz, *B*H_3).

Fig S1. ^{1}H (a), $^{13}C\{^{1}H\}$ (b) and ^{11}B (c) NMR spectra for compound **1** in C_6D_6.

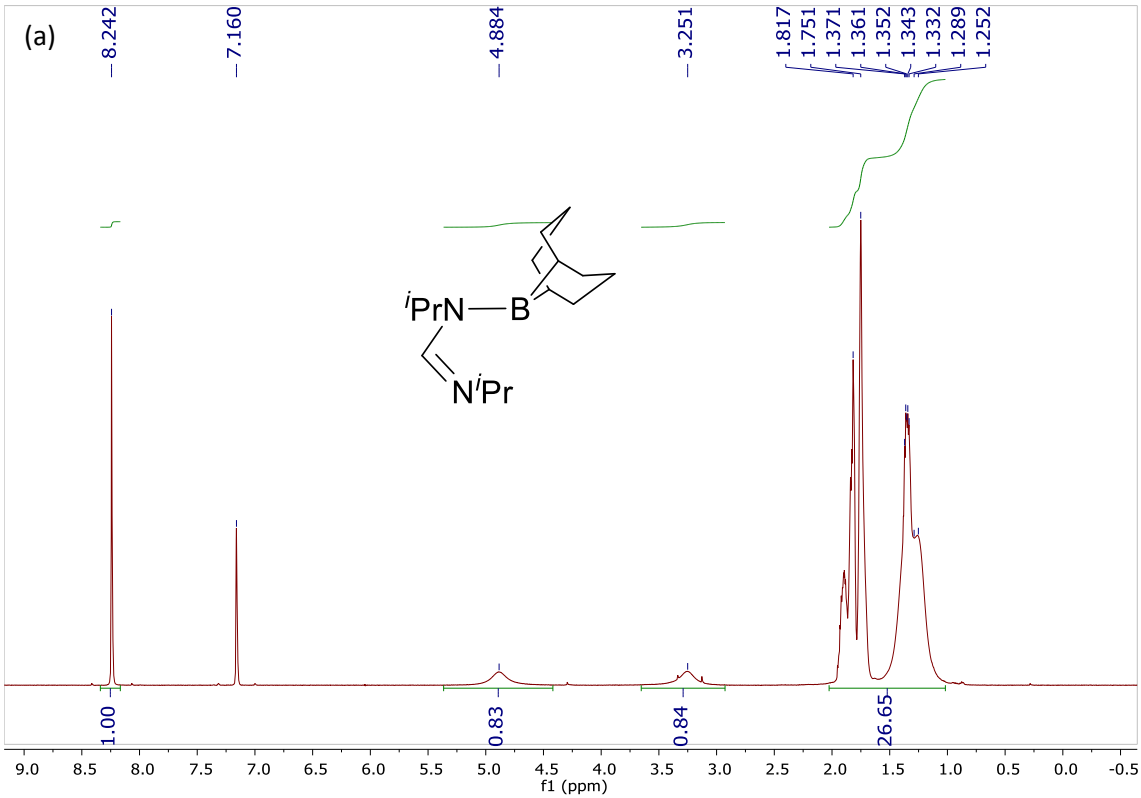

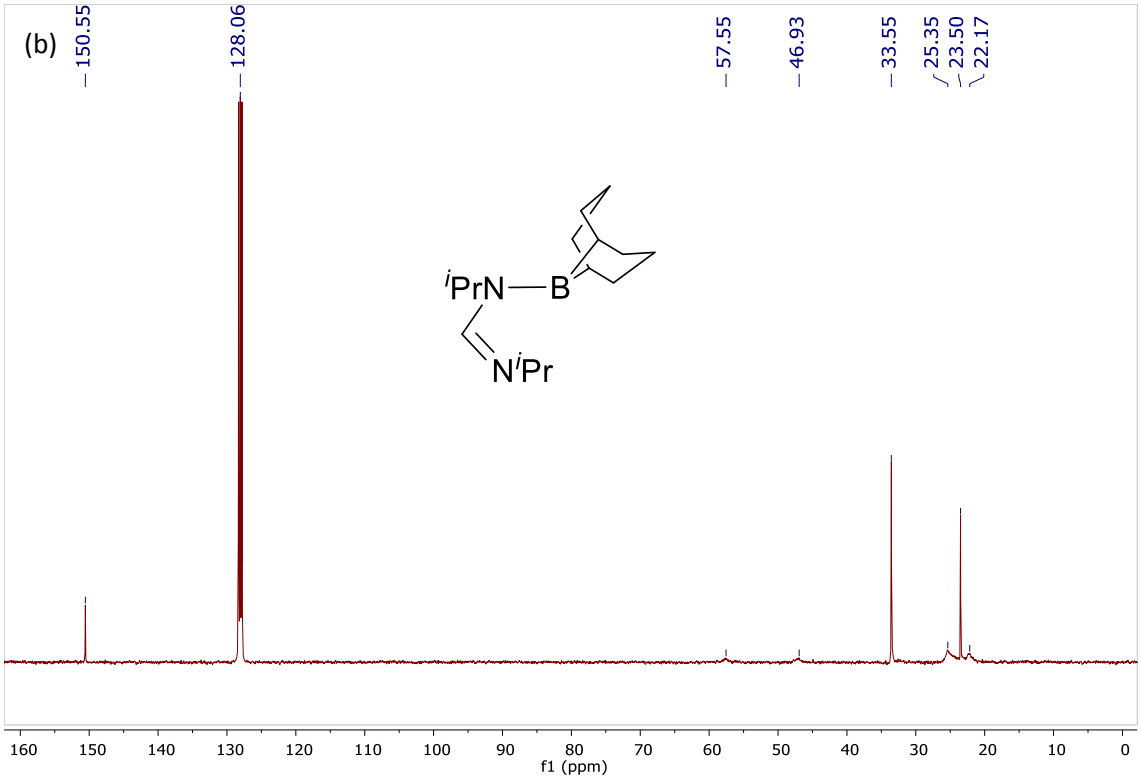

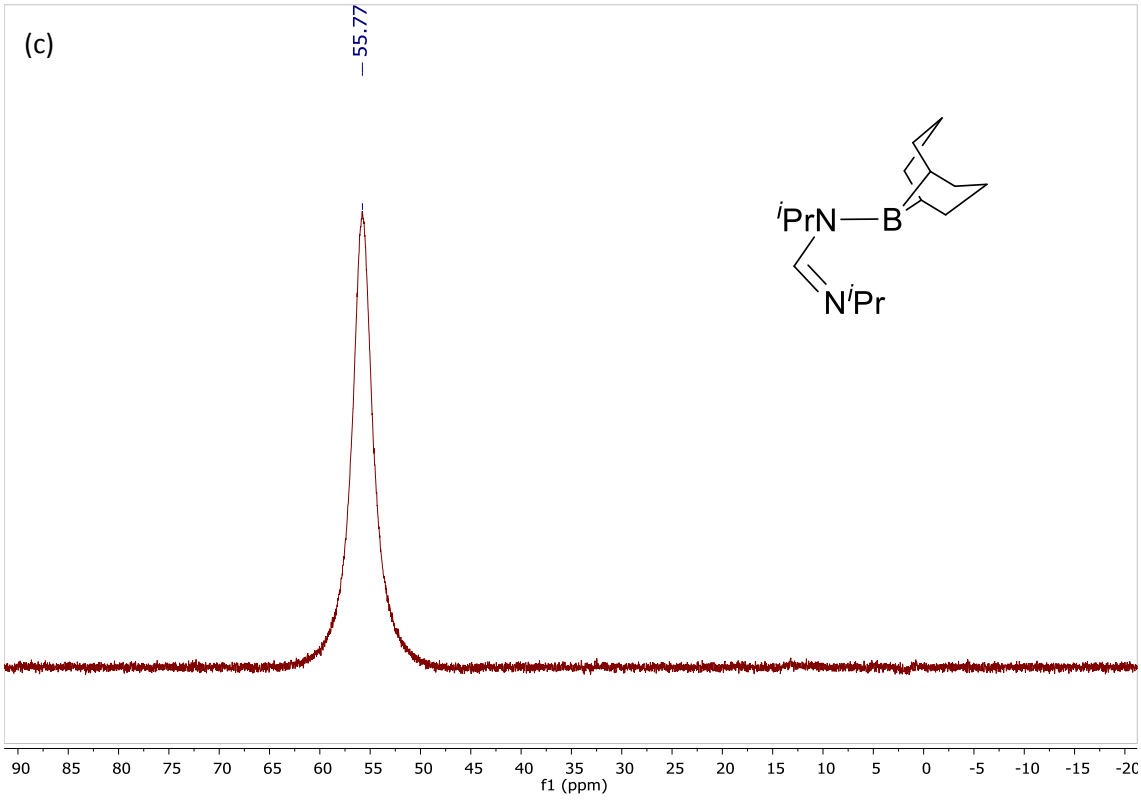
(c)
55.77
iPrN—B
NiPr
90 85 80 75 70 65 60 55 50 45 40 35 30 25 20 15 10 5 0 -5 -10 -15 -20
f1 (ppm)

Fig S2. ^{1}H (a), $^{13}C\{^{1}H\}$ (b) and ^{11}B (c) NMR spectra for compound **2** in C_6D_6, in equilibrium with **1** (°) and H-BC_8H_{14} (*).

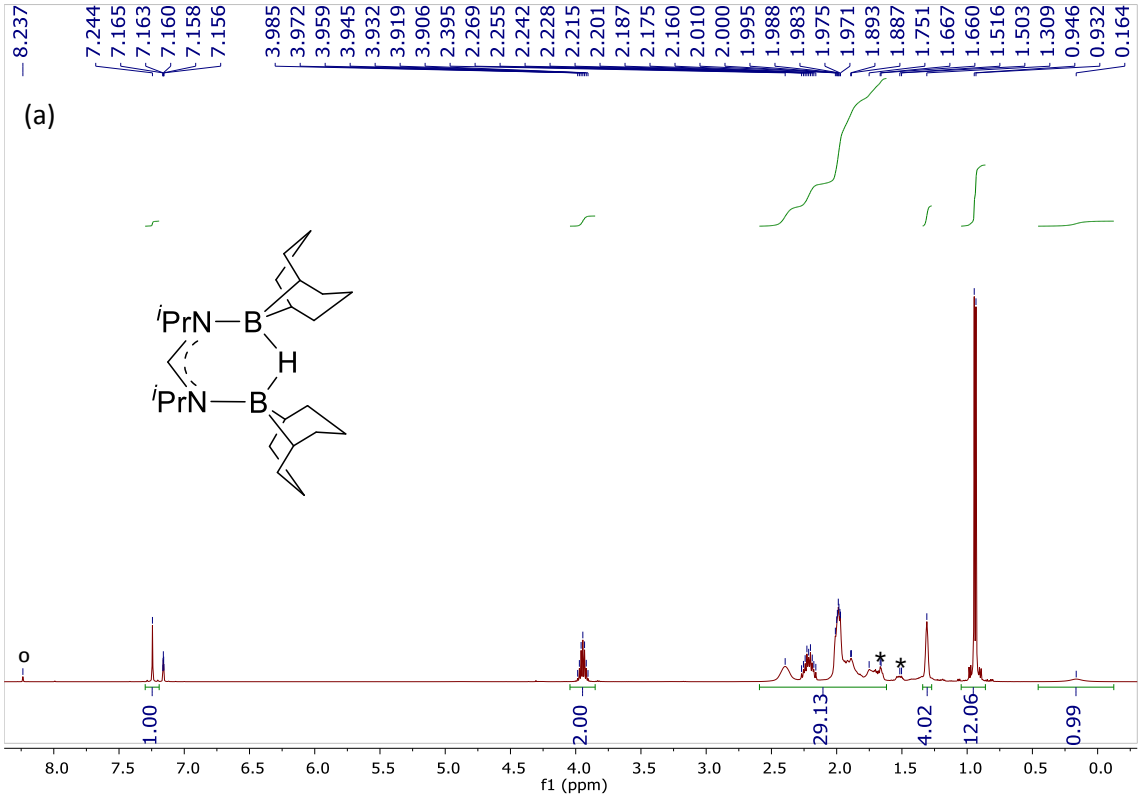

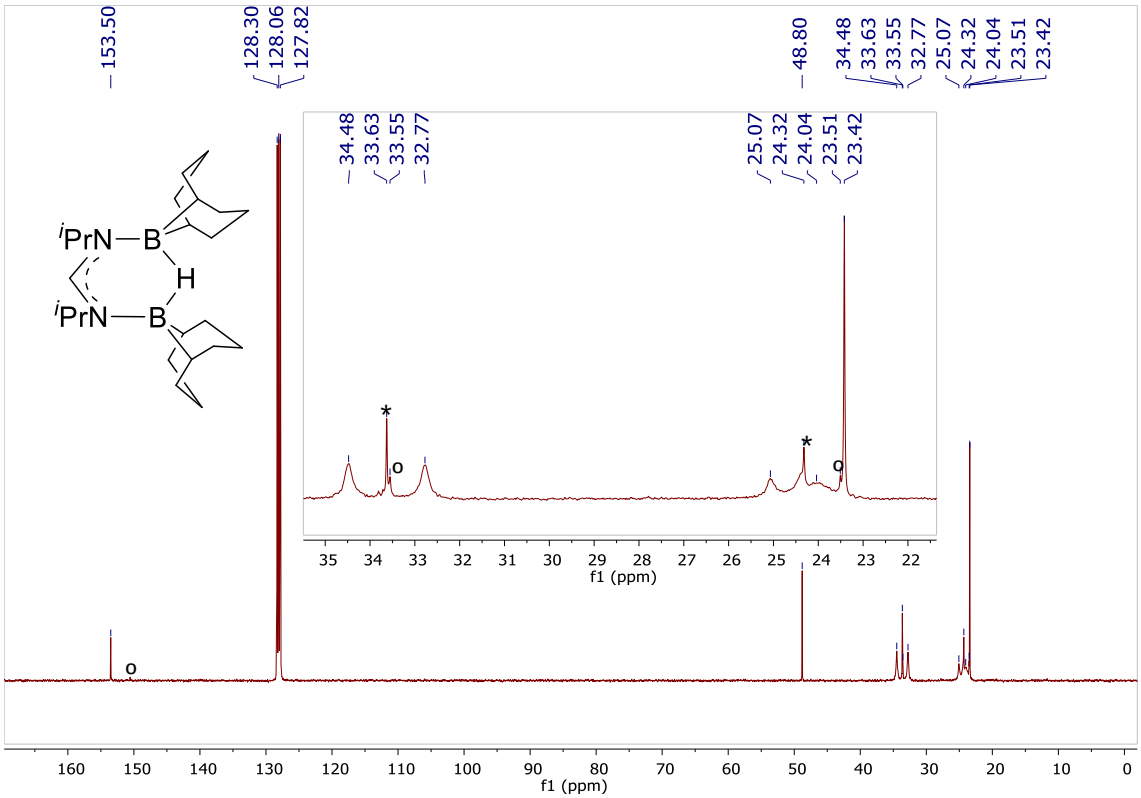

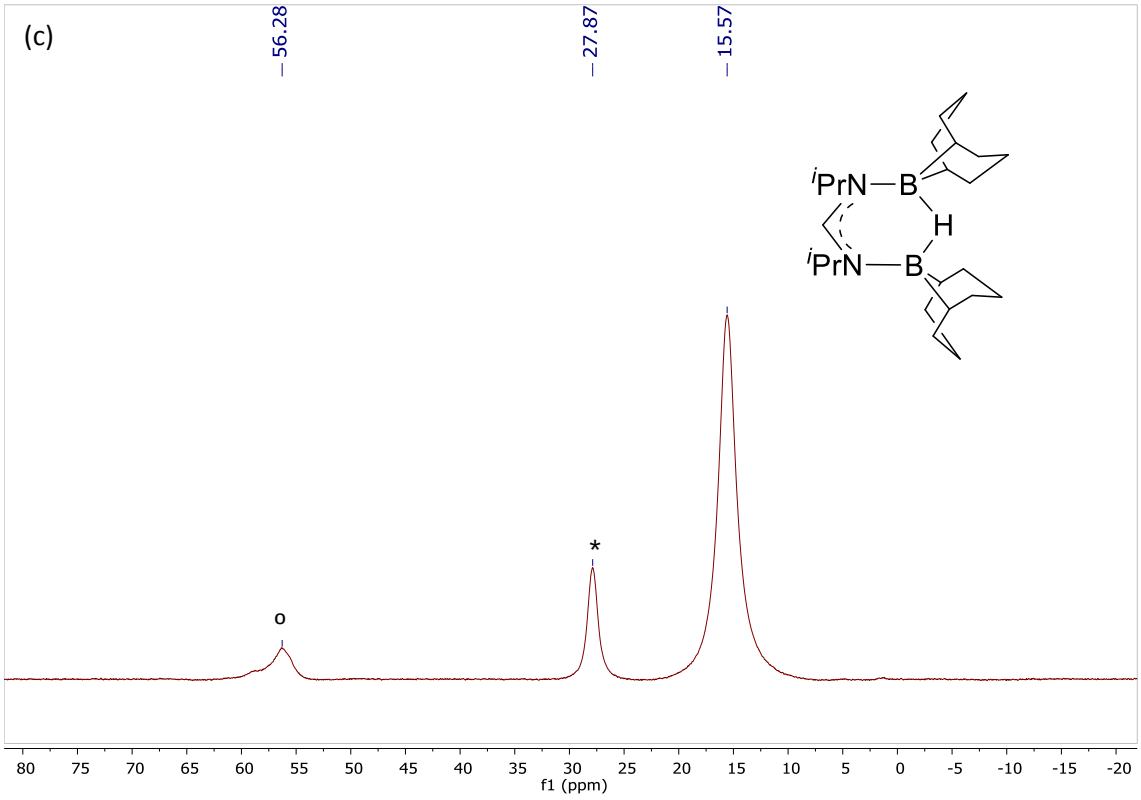
(c)
56.28
27.87
15.57
iPrN—B
H
iPrN—B
o
*
80 75 70 65 60 55 50 45 40 35 30 25 20 15 10 5 0 -5 -10 -15 -20
f1 (ppm)

Fig S3. ^{1}H (a) and ^{11}B (b) NMR stack plots of the equilibrium between compounds **2**, **1** (º) and H-BC_8H_{14} (*) at 25 and 60 ºC in C_6D_6.

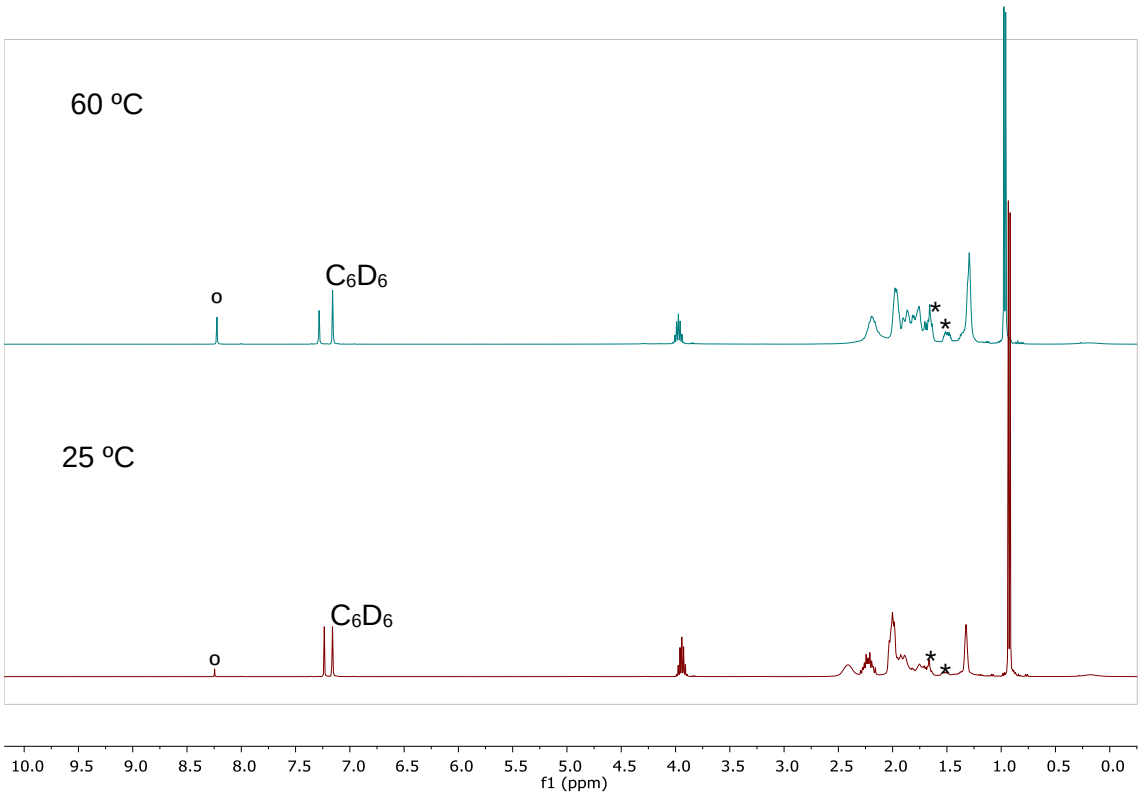

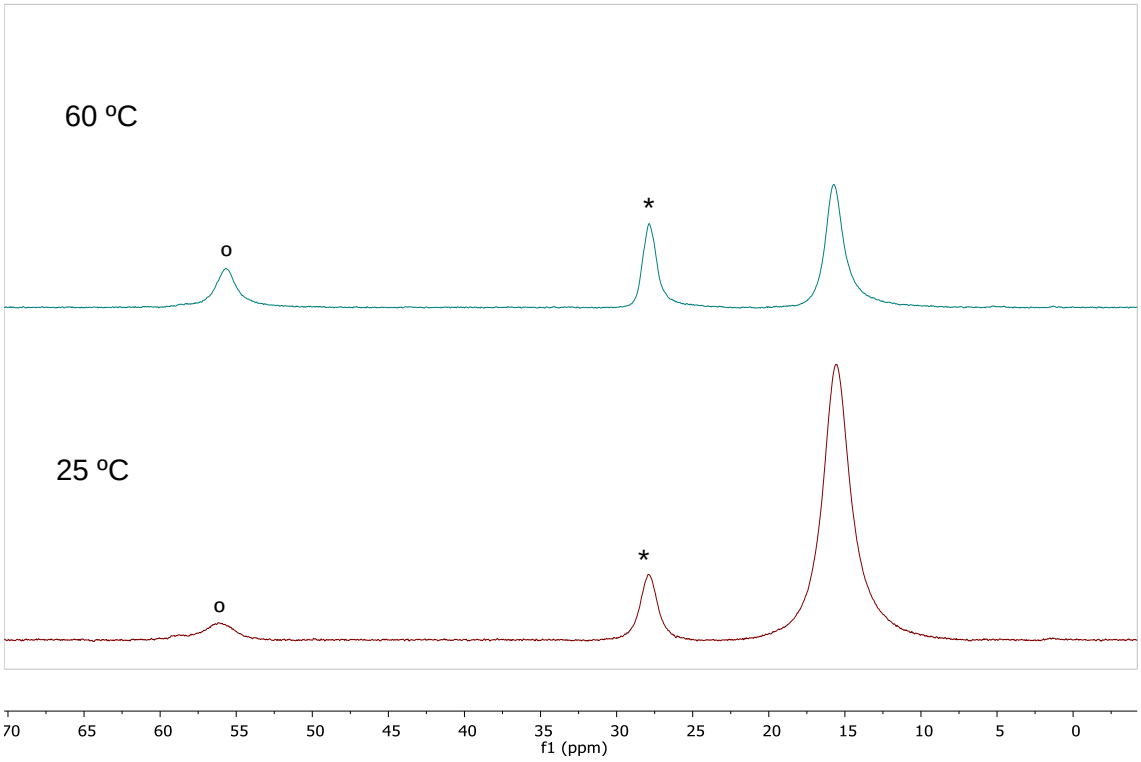

Fig S4. ^{1}H (a), $^{13}C\{^{1}H\}$ (b) and ^{11}B (c) NMR spectra for compound **3** in CD_2Cl_2.

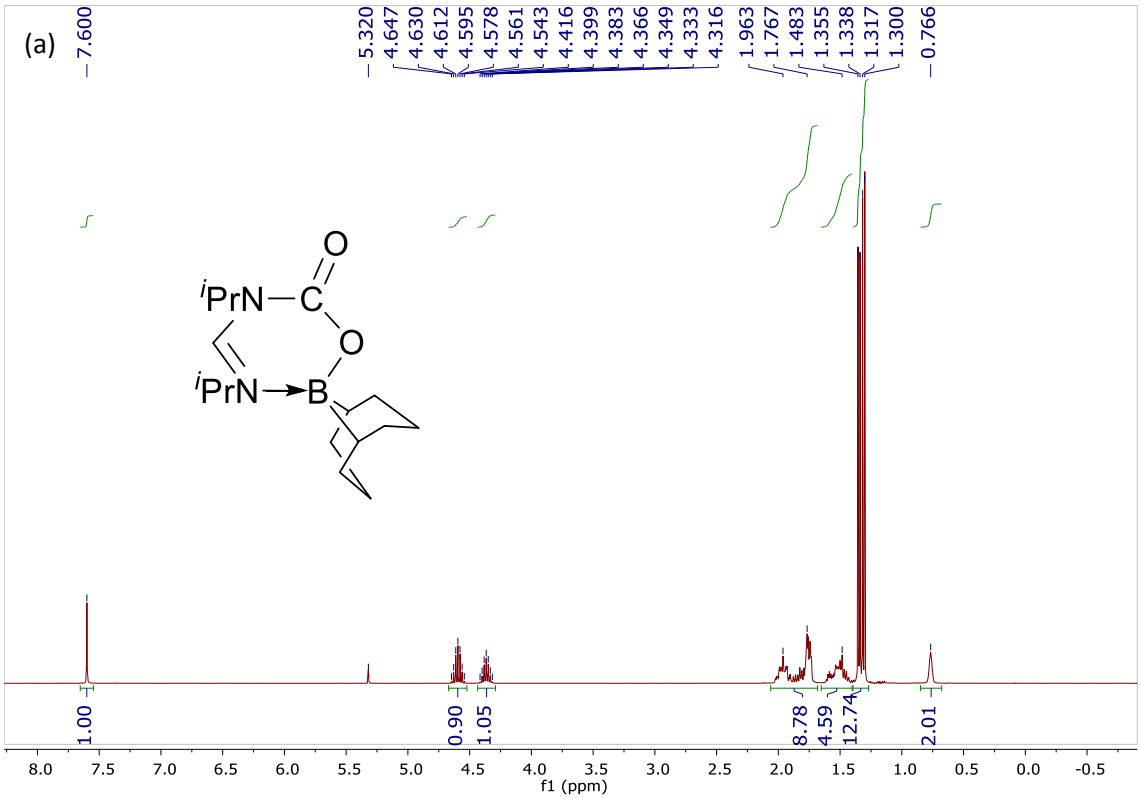

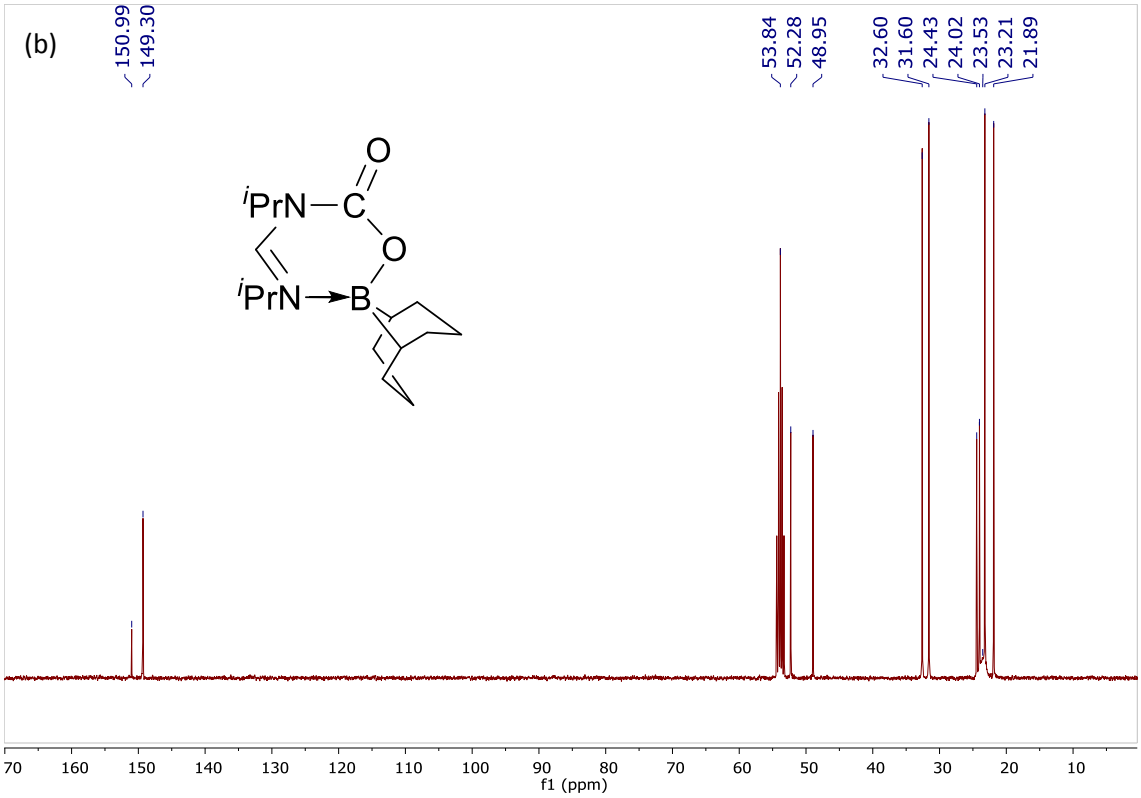

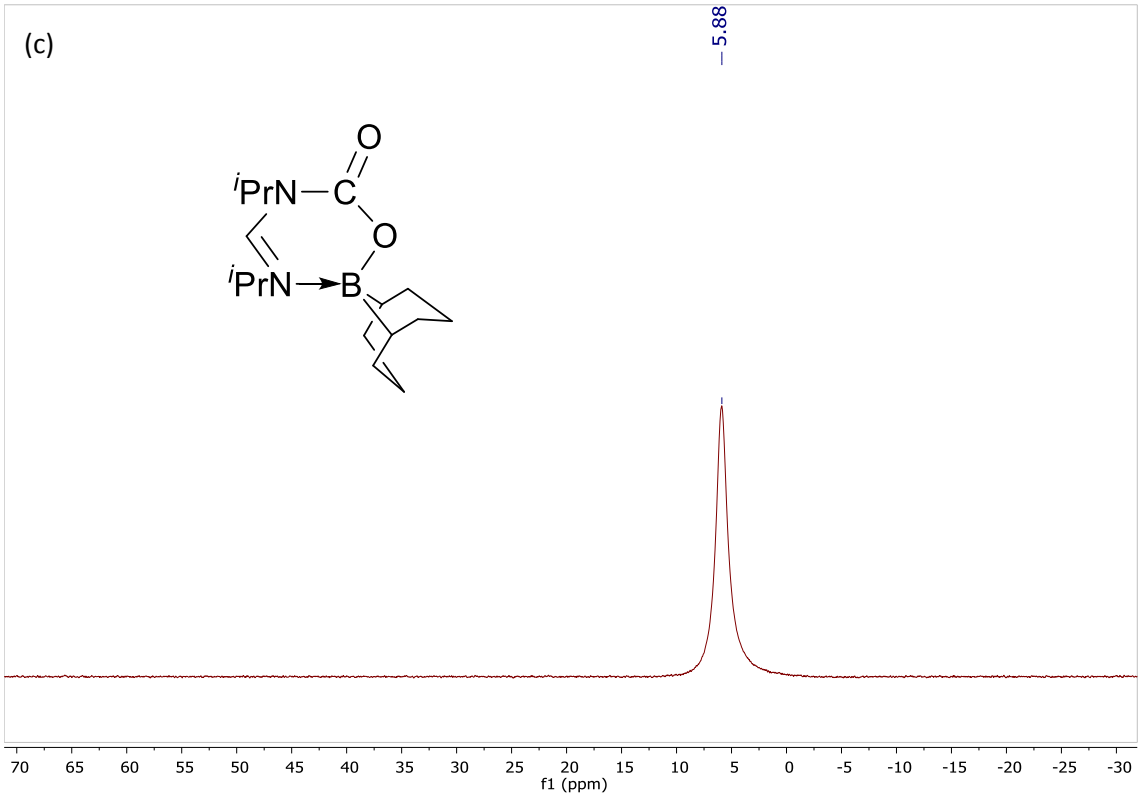
(c)
5.88
O
iPrN—C
O
iPrN→B
70 65 60 55 50 45 40 35 30 25 20 15 10 5 0 -5 -10 -15 -20 -25 -30
f1 (ppm)

Fig S5. ^{1}H (a), $^{13}C\{^{1}H\}$ (b) and ^{11}B (c) NMR spectra for compound **4** in C_6D_6.

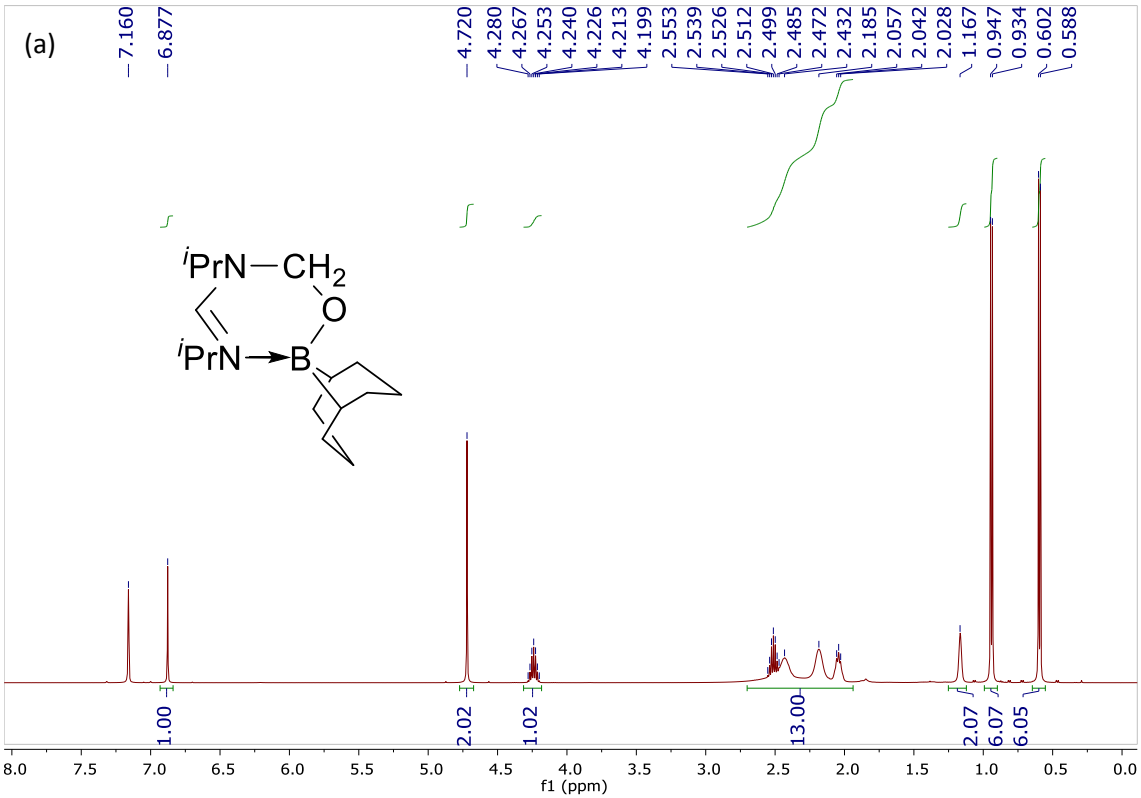

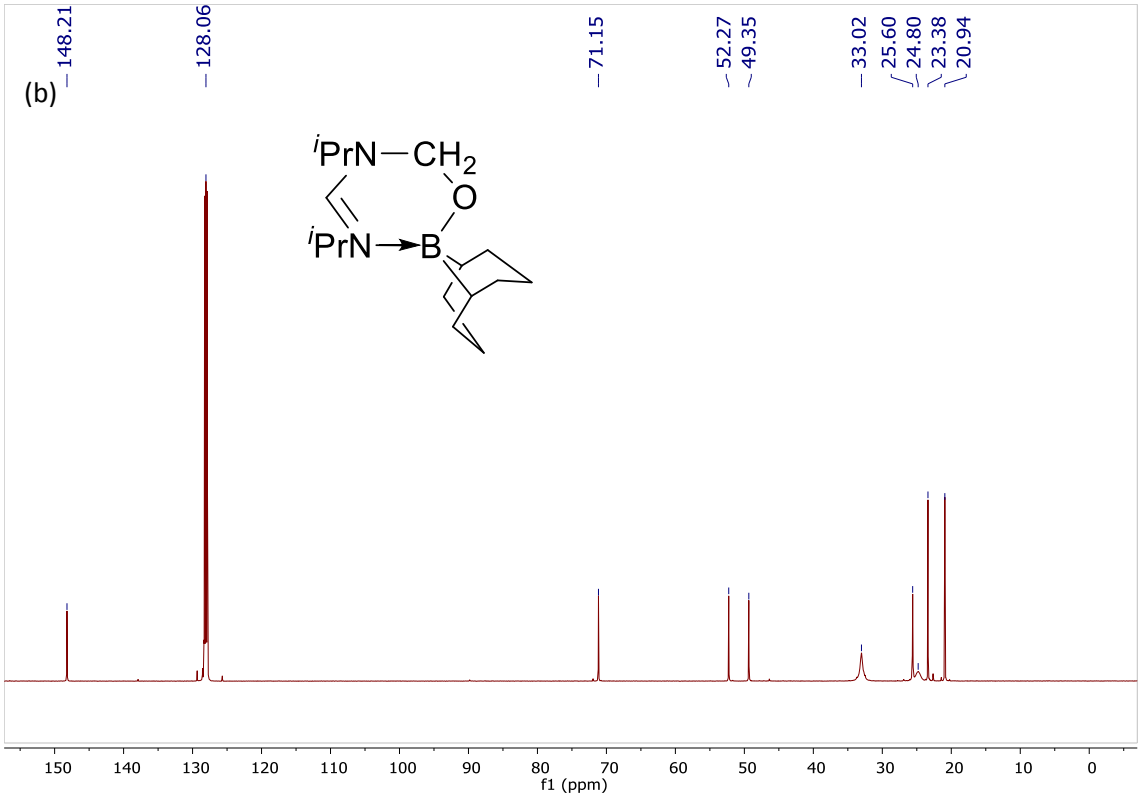

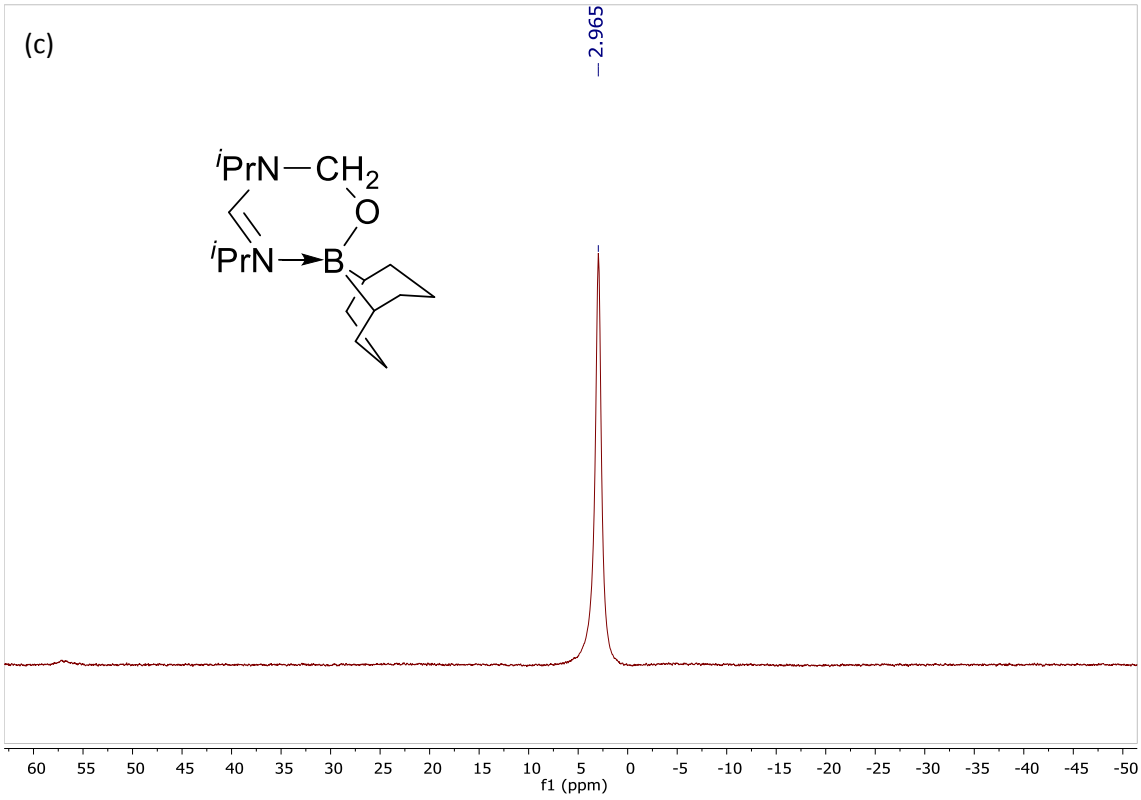
(c)
2.965
iPrN—CH2
O
iPrN→B
60 55 50 45 40 35 30 25 20 15 10 5 0 -5 -10 -15 -20 -25 -30 -35 -40 -45 -50
f1 (ppm)

Fig S6. ^{1}H (a) and ^{11}B (b) NMR spectra for the reaction of compound **3** (º) with 4 eq of H-BC_8H_{14} to give a mixture of **2** (*), **3** (º), **4** (+) and $O(B\ C_8H_{14})_2$ (3 days, 60 ºC, C_6D_6).

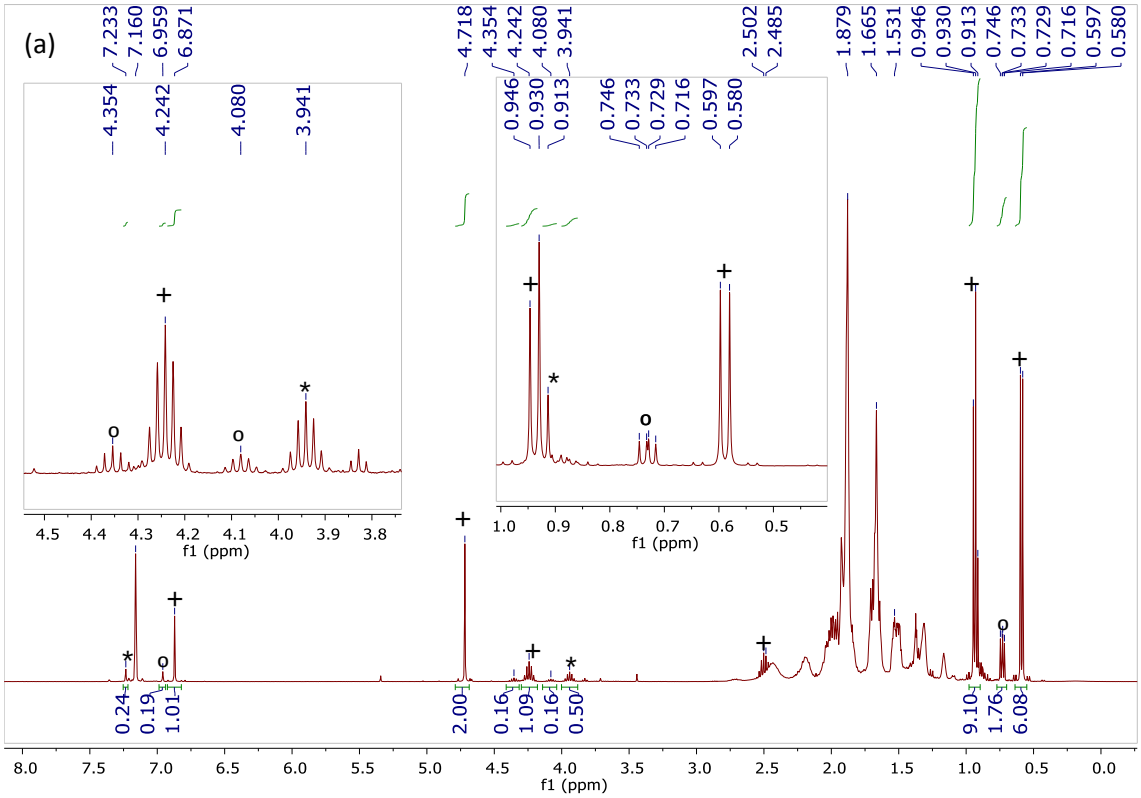

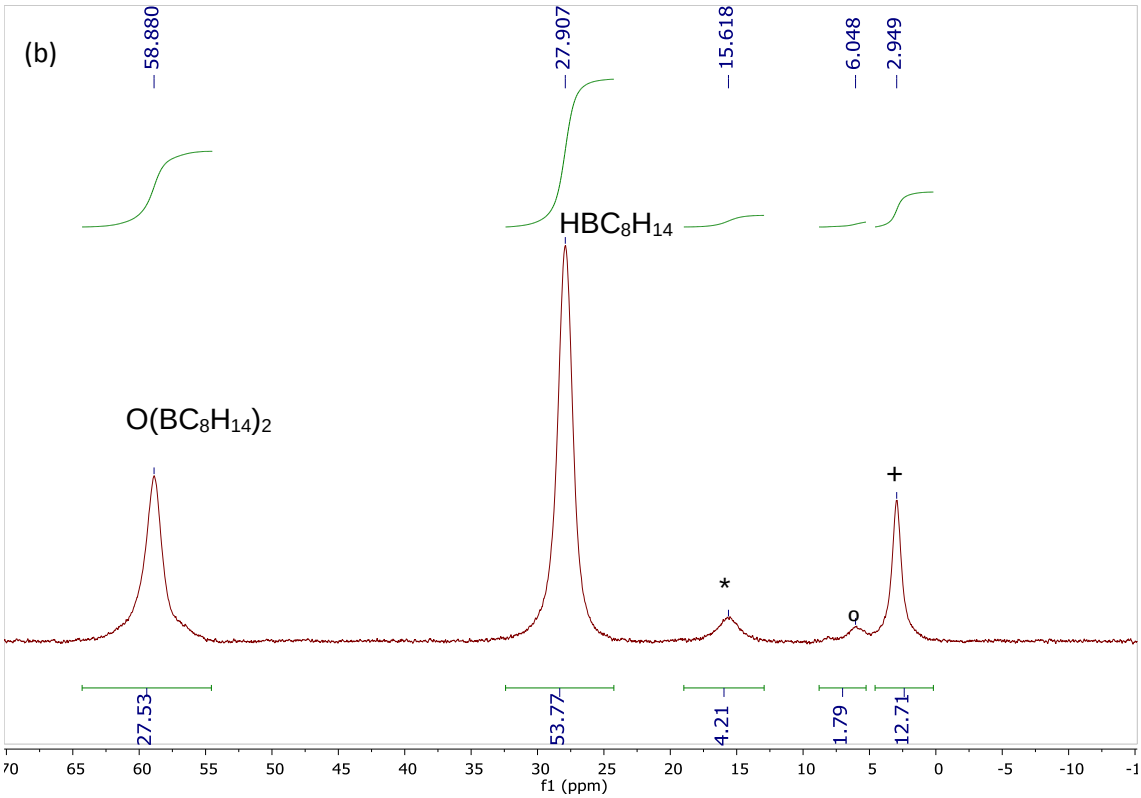

Fig S7. ^{1}H (a), $^{1}H\{^{11}B\}$ (b), $^{13}C\{^{1}H\}$ (c) and ^{11}B (d) NMR spectra for compound **5** in C_6D_6.

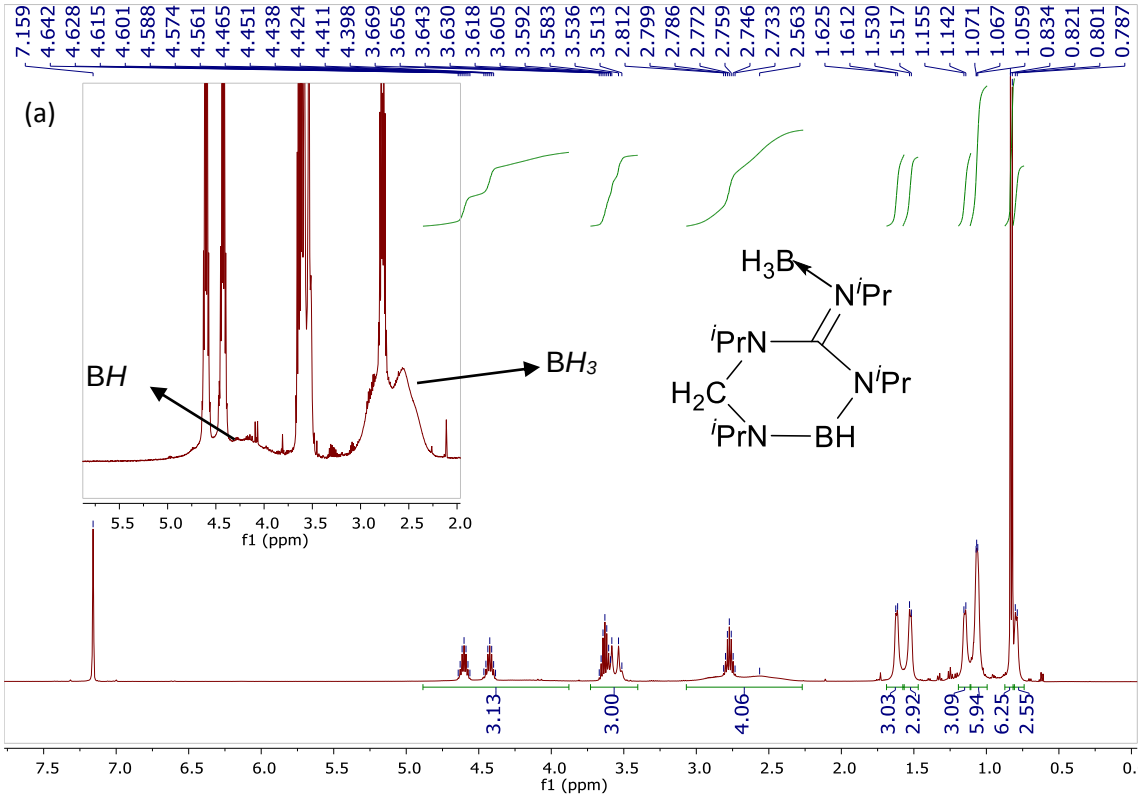

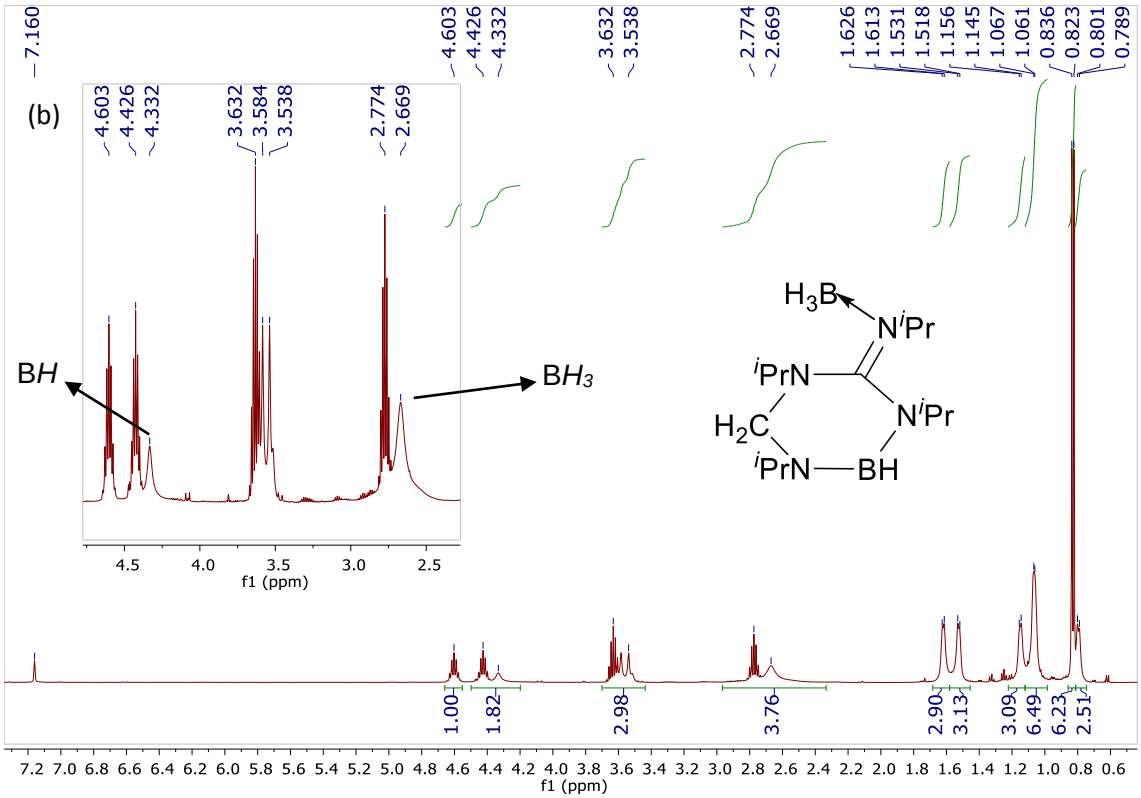

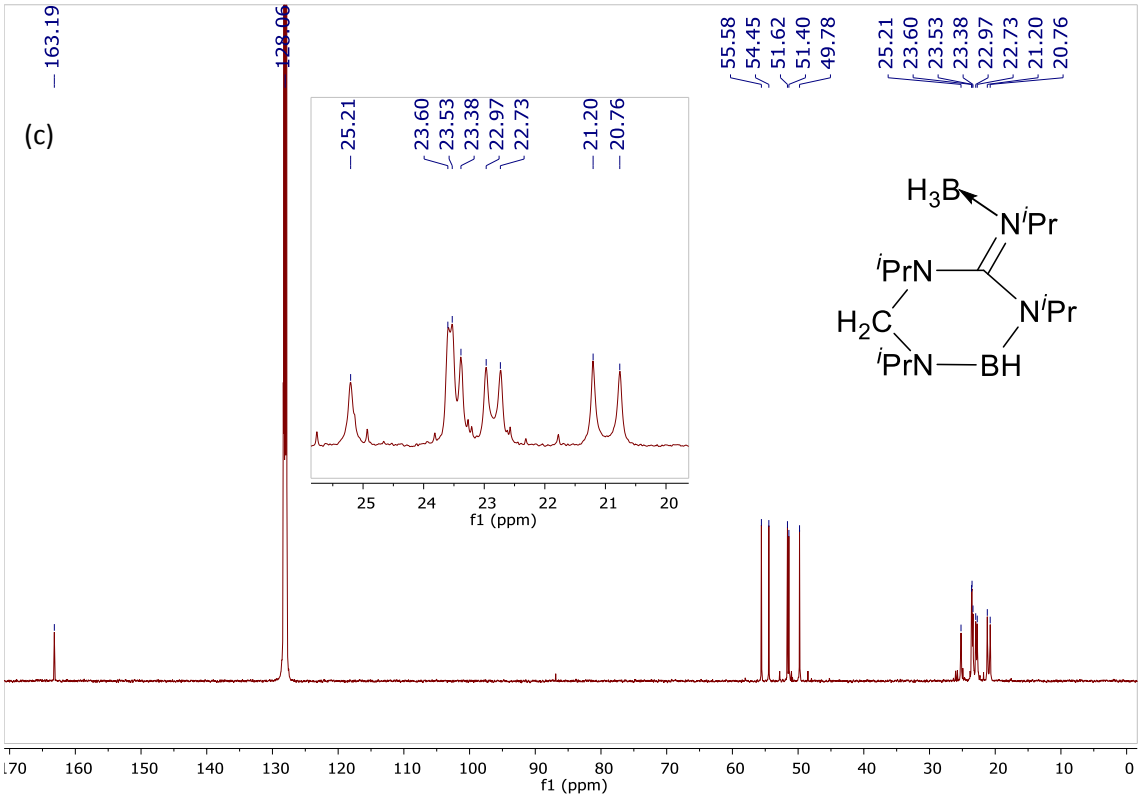
(c)
163.19
128.96
55.58
54.45
51.62
51.40
49.78
25.21
23.60
23.53
23.38
22.97
22.73
21.20
20.76
H_3B
N^iPr
^{i}PrN
N^iPr
H_2C
^{i}PrN
BH
f1 (ppm)

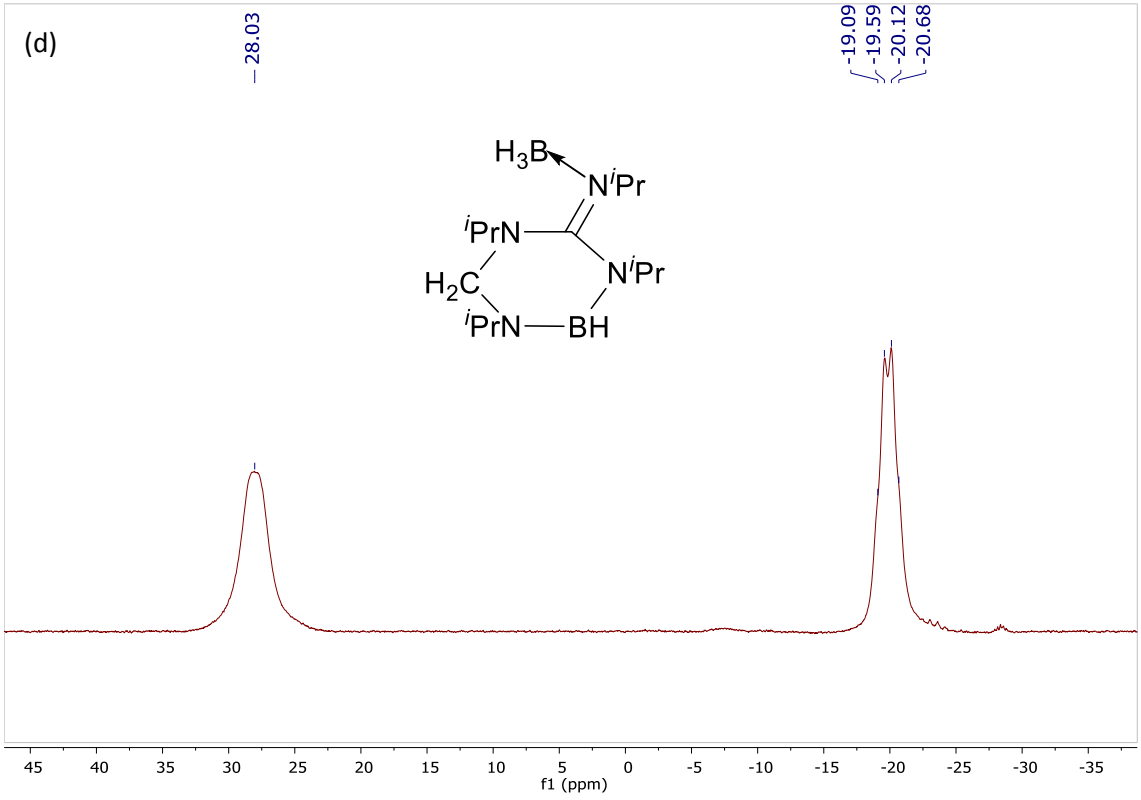
(d)
28.03
-19.09
-19.59
-20.12
-20.68
H_3B
N^iPr
^{i}PrN
N^iPr
H_2C
^{i}PrN
BH
f1 (ppm)

Catalytic reduction of $^{13}CO_2$ with H-BC_8H_{14}. In a glovebox, H-BC_8H_{14} (0.025 g, 0.20 mmol) was dissolved in 450 μL of C_6D_6 and charged to a NMR tube equipped with a J. Young valve. Subsequently, 50 μL of a 0.2 M stock solution in C_6D_6 of tetrakis(trimethylsilyl)silane (TKS, 0.01 mmol), used as an internal standard, were added to the NMR tube, followed by 50 μL of a 0.2 M stock solution of DIC or **4** in C_6D_6 (5 mol%), amounting to a final volume of ca. 0.55 mL. Afterwards, the NMR tube was subjected to a freeze-pump-thaw cycle: frozen with liquid N_2, evacuated under vacuum and refilled with $^{13}CO_2$ (*ca*. 1 atm) after reaching room temperature. Then, the sample was thoroughly shaken, placed in an oil bath at 60 ºC and monitored by multinuclear NMR. The chemical shifts of the reduction products in the ^{1}H, ^{13}C and ^{11}B NMR spectra compare well with those reported in the literature.[1] The TON was calculated according to the number of C-H formed in the reduction products by integration of the corresponding signals in the ^{1}H NMR spectrum relative to the internal standard. After 20 h, >97% of the borane was consumed.

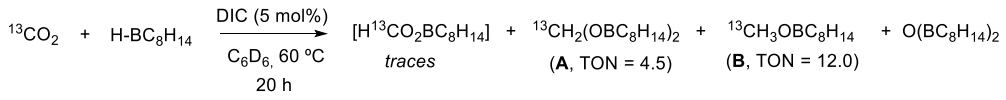

Fig S8. ^{1}H (a), ^{13}C{^{1}H} (b) and ^{11}B (c) NMR spectra for the reduction of $^{13}CO_2$ with H-BC_8H_{14} catalysed by DIC.

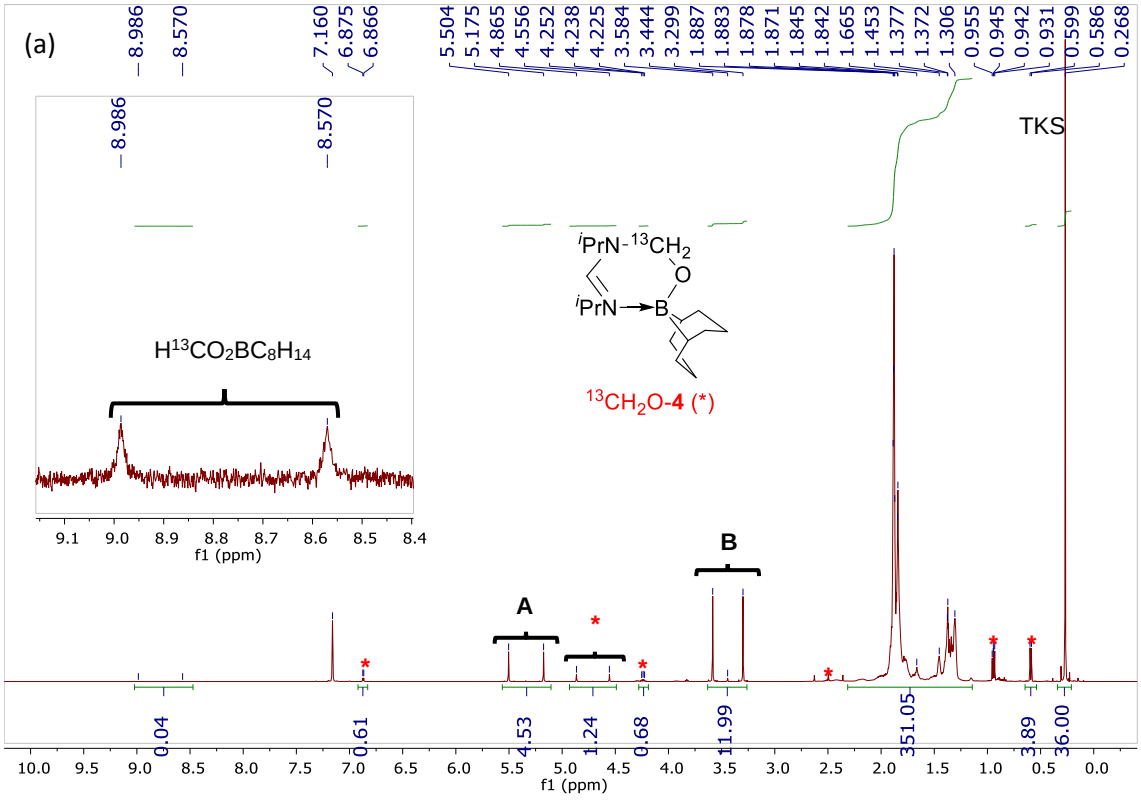

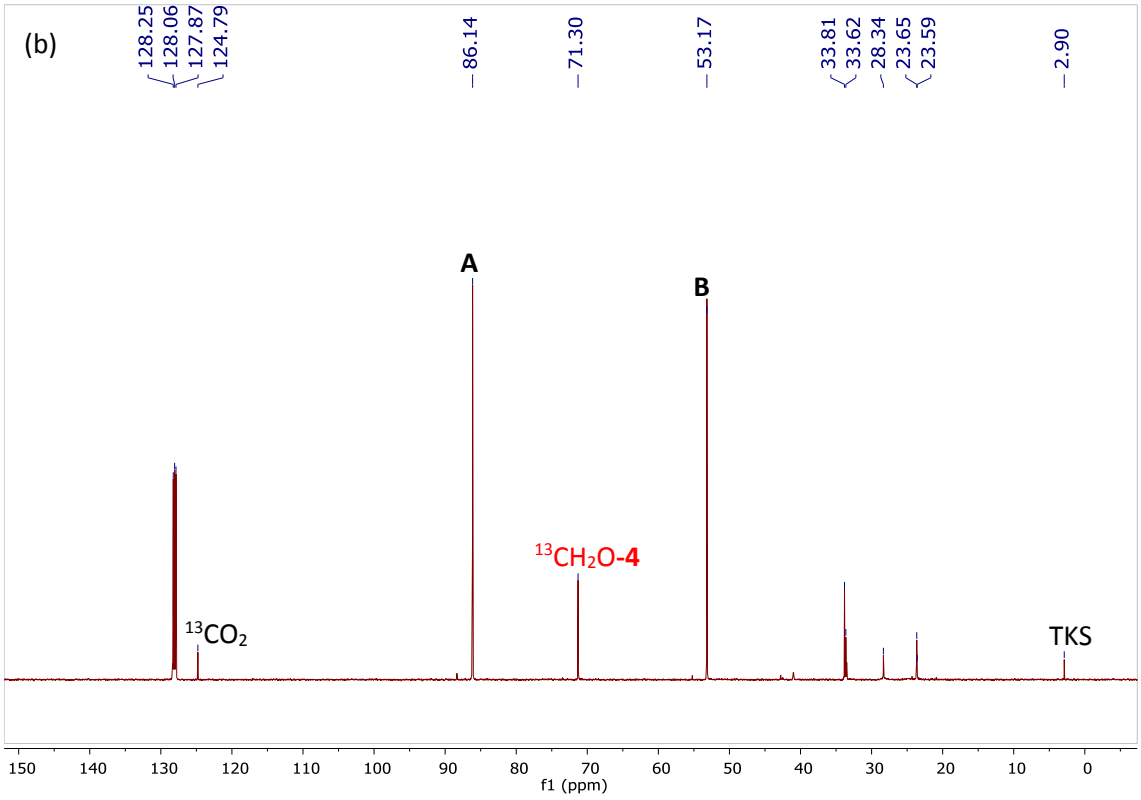
(b)
128.25
128.06
127.87
124.79
86.14
71.30
53.17
33.81
33.62
28.34
23.65
23.59
2.90
A
B
$^{13}CH_2O$-4
$^{13}CO_2$
TKS
f1 (ppm)

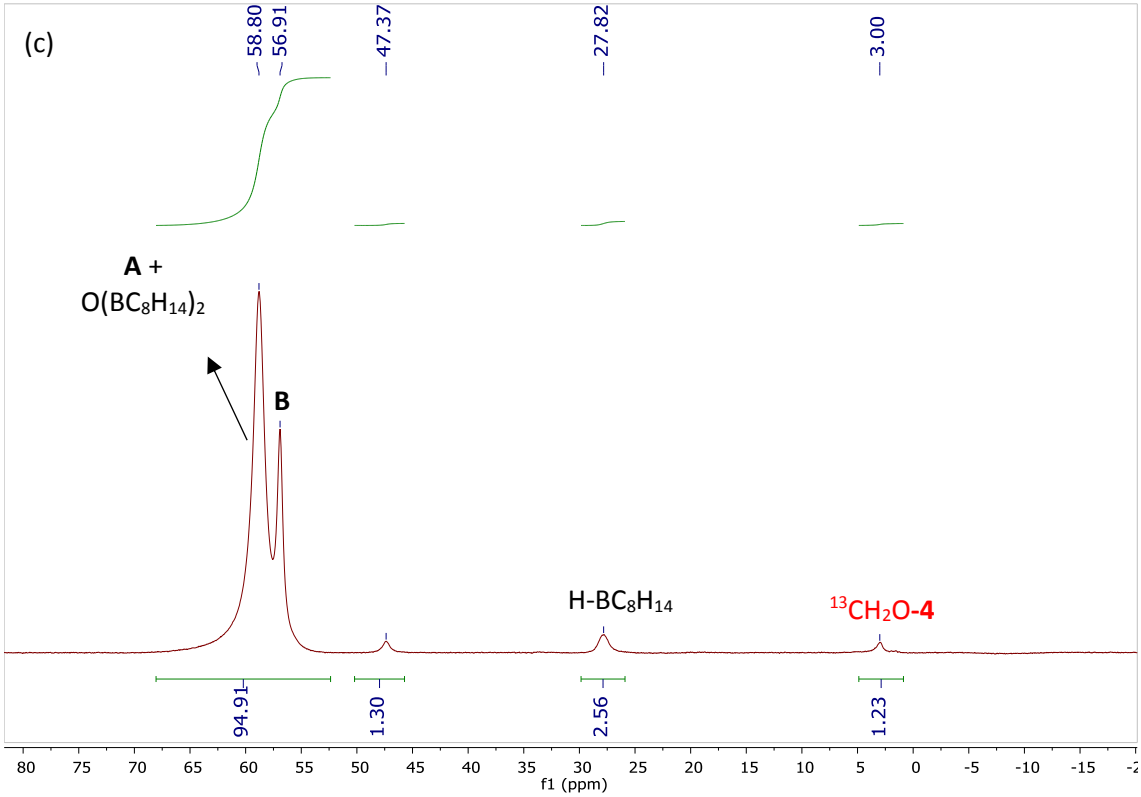
(c)
58.80
56.91
47.37
27.82
3.00
A +
$O(BC_8H_{14})_2$
B
H-BC_8H_{14}
$^{13}CH_2O$-4
94.91
1.30
2.56
1.23
f1 (ppm)

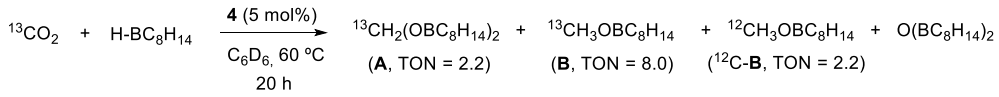

Fig S9. ^{1}H (a), $^{13}C\{^{1}H\}$ (b) and ^{11}B (c) NMR spectra for the reduction of $^{13}CO_2$ with H-BC_8H_{14} catalysed by **4**.

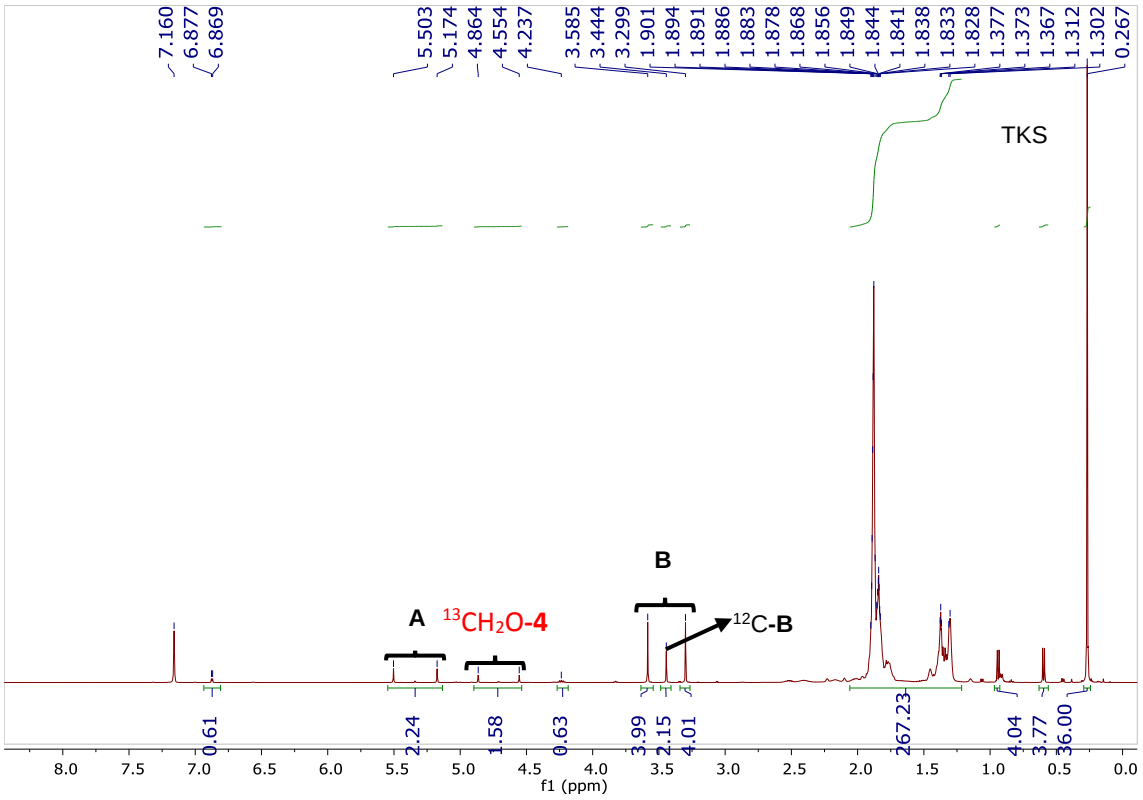

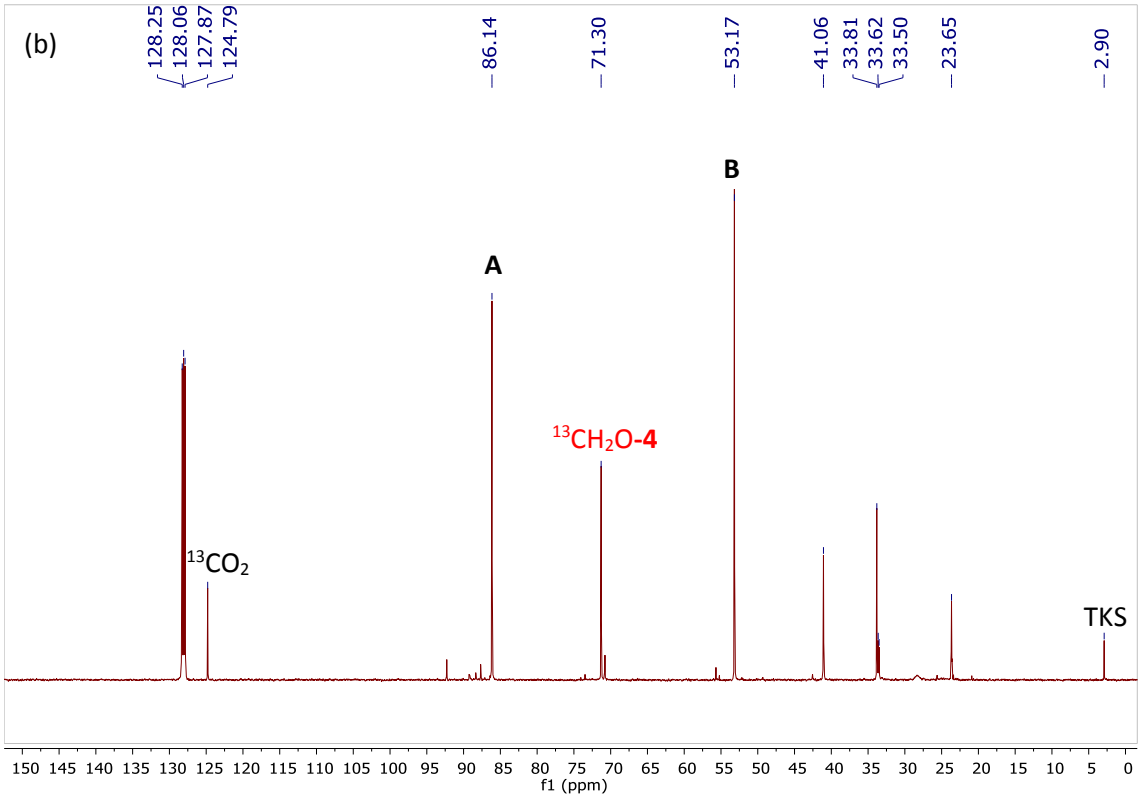
(b)
128.25
128.06
127.87
124.79
86.14
71.30
53.17
41.06
33.81
33.62
33.50
23.65
2.90
A
B
$^{13}CH_2O$-4
$^{13}CO_2$
TKS
150 145 140 135 130 125 120 115 110 105 100 95 90 85 80 75 70 65 60 55 50 45 40 35 30 25 20 15 10 5 0
f1 (ppm)

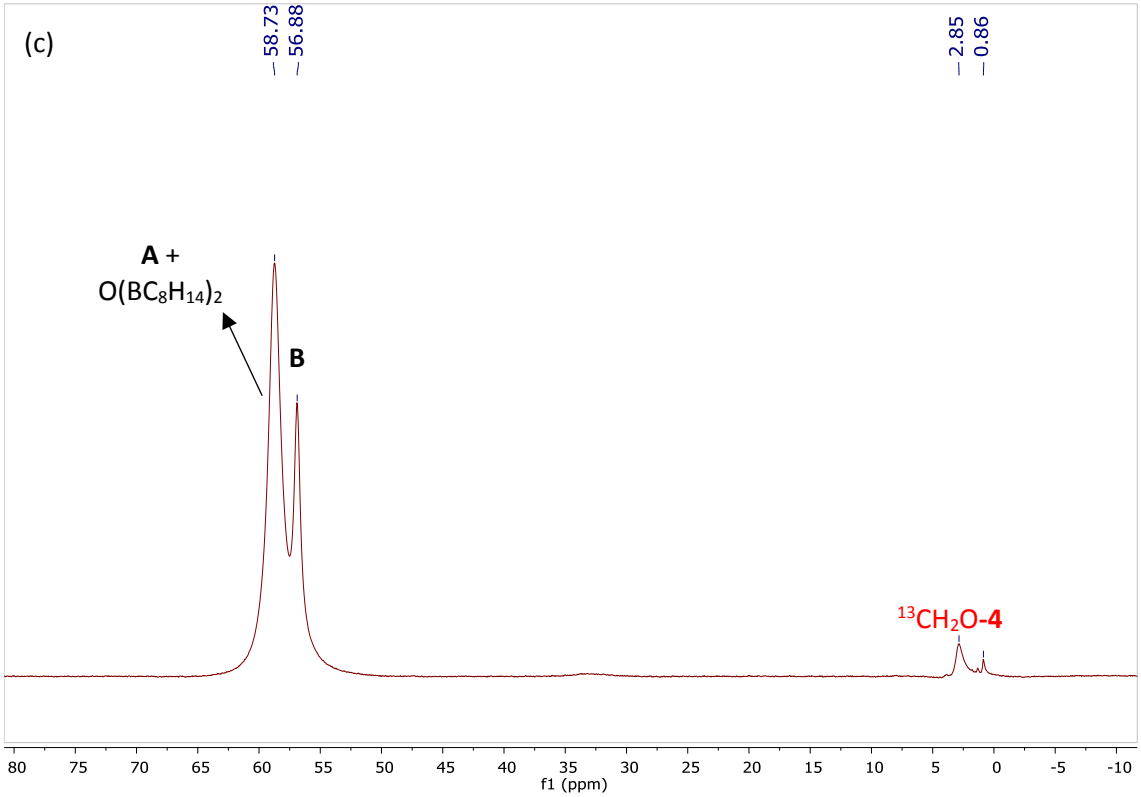
(c)
58.73
56.88
2.85
0.86
A +
$O(BC_8H_{14})_2$
B
$^{13}CH_2O$-4
80 75 70 65 60 55 50 45 40 35 30 25 20 15 10 5 0 -5 -10
f1 (ppm)

Typical procedure for the catalytic reduction of CO_2 with H-BC_8H_{14}. In a glovebox, H-BC_8H_{14} (0.025 g, 0.20 mmol) was dissolved in 450-500 μL of C_6D_6 and charged to a NMR tube equipped with a J. Young valve. Subsequently, 50 μL of a 0.2 M stock solution in C_6D_6 of TKS (0.01 mmol), used as an internal standard, were added to the NMR tube, followed by the adequate volume of a 0.2 M stock solution of the catalyst in C_6D_6, amounting to a final volume of ca. 0.55 mL. Afterwards, the NMR tube was connected to a vacuum / CO_2 line and subjected to a freeze-pump-thaw cycle: frozen with liquid N_2, evacuated under vacuum and refilled with CO_2 (*ca.* 1 atm) after reaching room temperature. Then, the sample was thoroughly shaken, kept at the desired temperature and monitored by multinuclear NMR. The chemical shifts of $CH_2(OBC_8H_{14})_2$ (**A**) and $CH_3OBC_8H_{14}$ (**B**) in the ^1H, ^{13}C and ^{11}B NMR spectra compared well with those reported in the literature.[1-2] The TON was calculated according to the number of C-H formed in the reduction products by integration of the corresponding signals relative to the internal standard. [Example: DIC (1 mol%), 60 ºC, 22h]

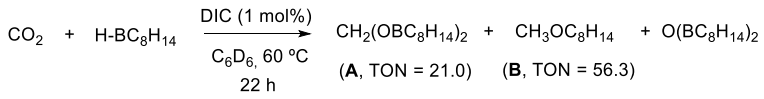

Fig S10. ^1H (a), and ^{11}B (b) NMR spectra for the catalytic reduction of CO_2 with H-BC_8H_{14}.

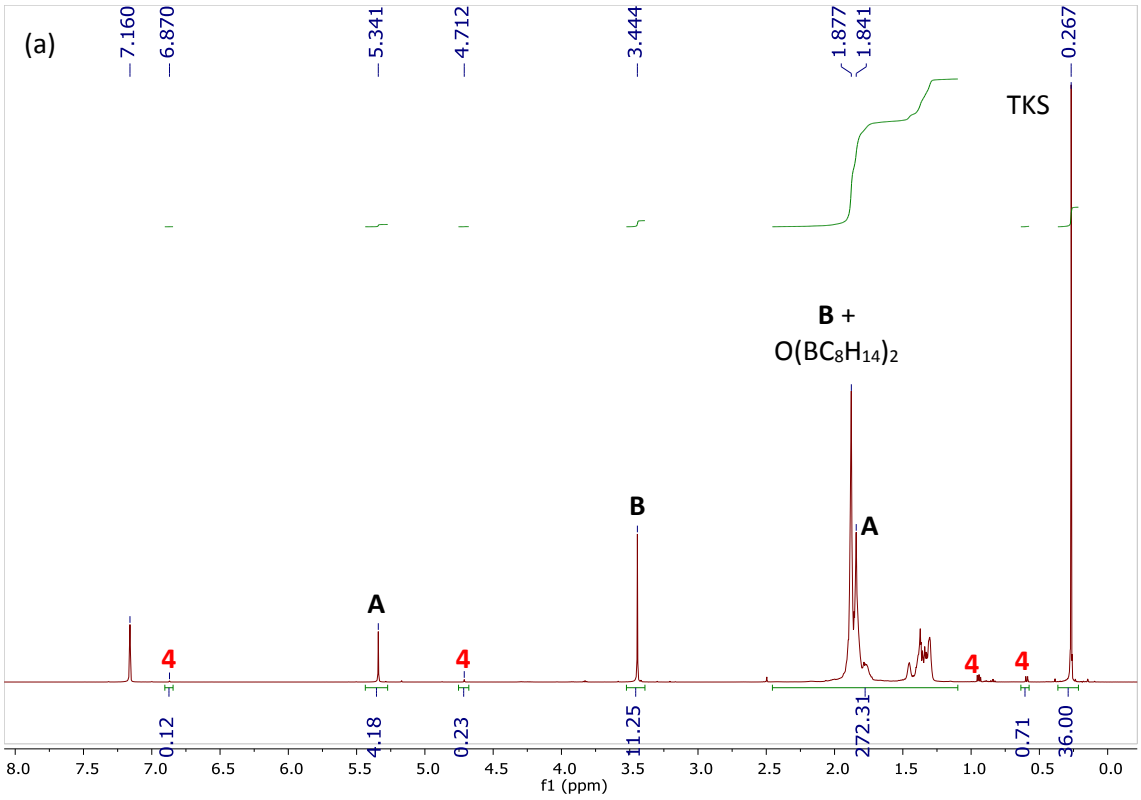

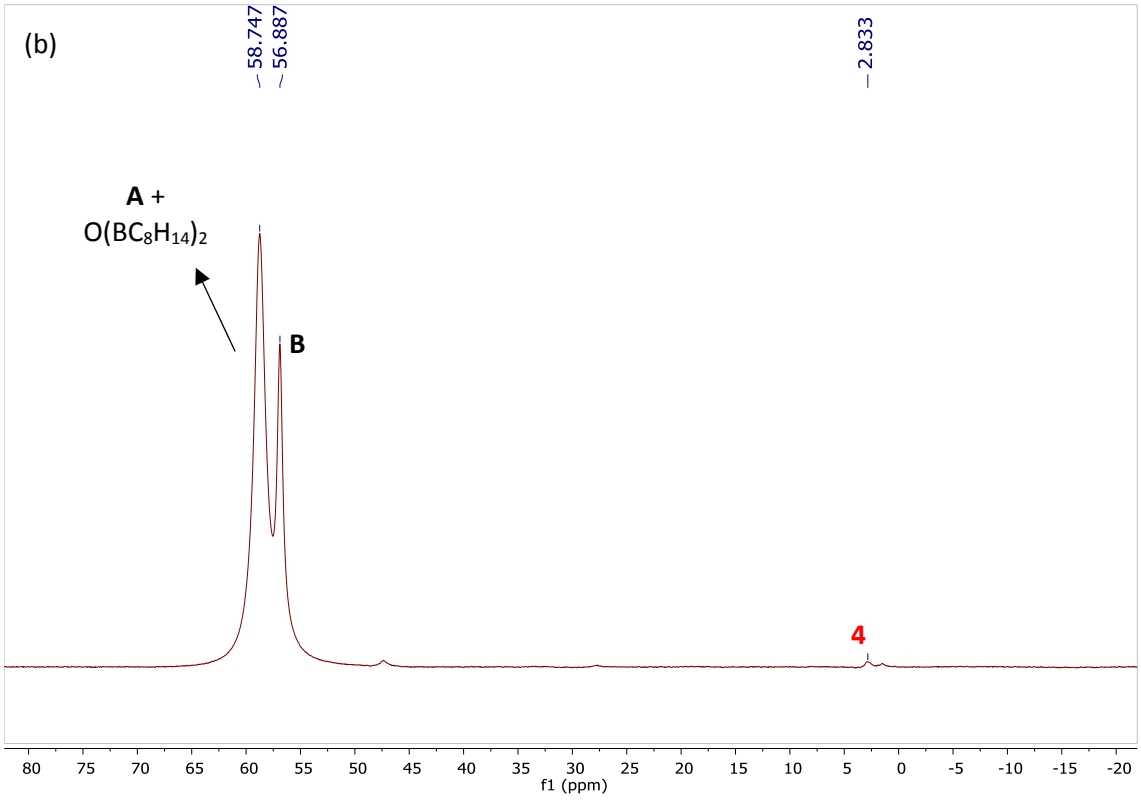
(b)
58.747
56.887
2.833
A +
O(BC8H14)2
B
4
80 75 70 65 60 55 50 45 40 35 30 25 20 15 10 5 0 -5 -10 -15 -20
f1 (ppm)

Typical procedure for the catalytic reduction of CO_2 with $BH_3{\cdot}SMe_2$. In a glovebox, $BH_3{\cdot}SMe_2$ (47.5 μL, 0.50 mmol) was dissolved in 500-600 μL of C_6D_6 in a 40 mL-schlenk equipped with a stir bar and a J. Young stopper. Then, 50 μL of a 0.2 M stock solution in C_6D_6 of TKS (0.01 mmol), used as an internal standard, and the adequate volume of a 0.2 M stock solution in C_6D_6 of the catalyst were added, amounting to a final volume *ca.* 0.7 mL. Afterwards, the schlenk tube was connected to a vacuum / CO_2 line and subjected to a freeze-pump-thaw cycle: frozen with liquid N_2, evacuated under vacuum and refilled with CO_2 (*ca.* 1 atm) upon melting. The solution was stirred at the desired temperature for a set period of time, after which it was checked by multinuclear NMR. The TON was calculated according to the number of C-H formed in the reduction products $[(CH_3O)BO]_3$ (**C**) and $B(OCH_3)_3$ (**D**) by integration of the corresponding signals in the ^1H NMR spectrum at 3.36 and 3.42 ppm, respectively, relative to the internal standard.[1b, 3] [Example: DIC (5 mol%), 24 h, 25 ºC]

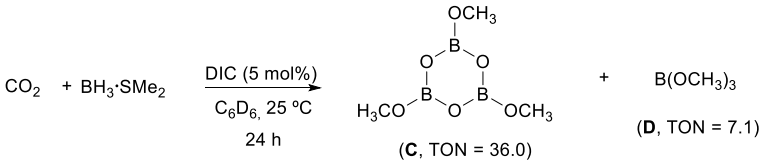

Fig S11. ^1H (a), $^{13}C\{^1H\}$ (b) and ^{11}B (c) NMR spectra for the reduction of CO_2 with BH_3.

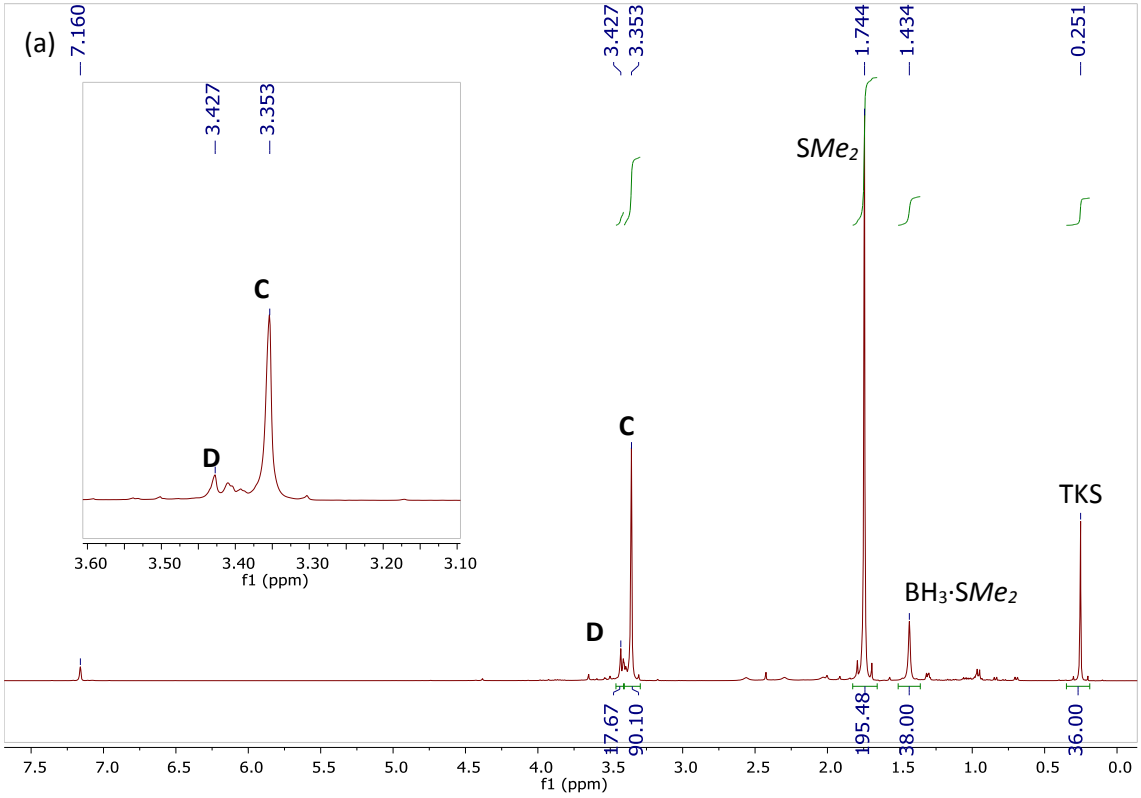

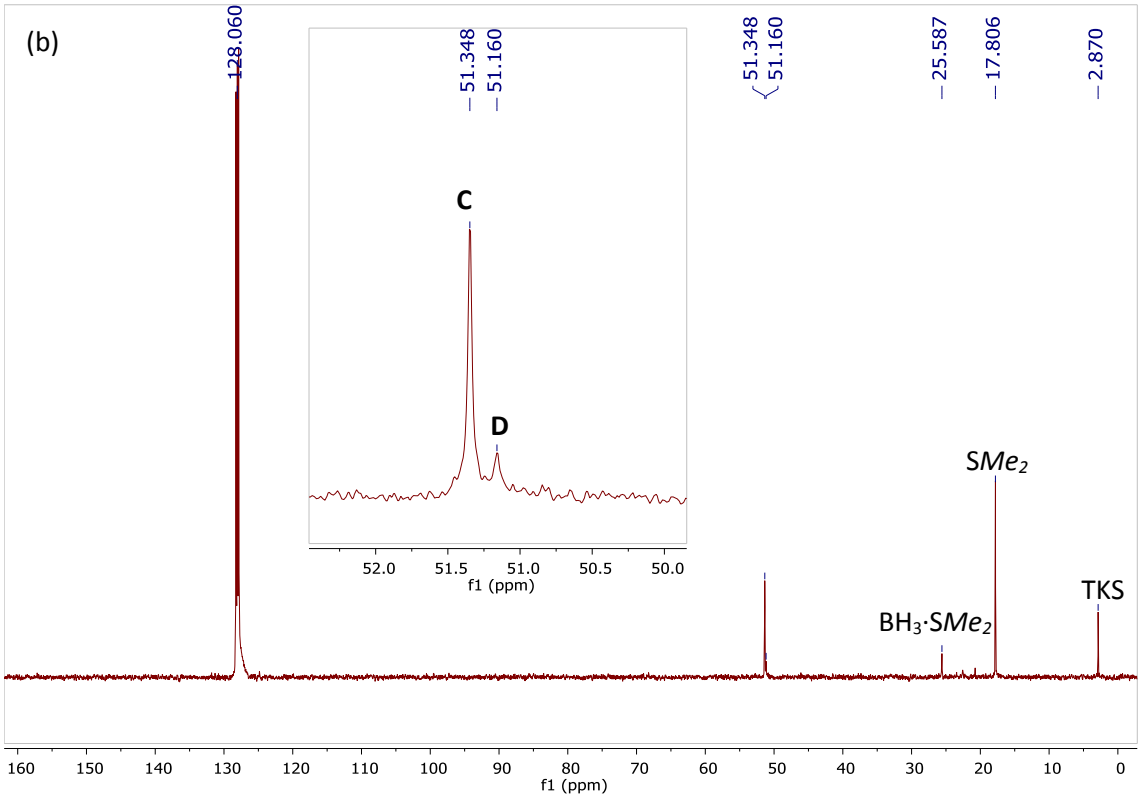
(b)
128.060
51.348
51.160
25.587
17.806
2.870
C
D
SMe2
TKS
BH3·SMe2
f1 (ppm)

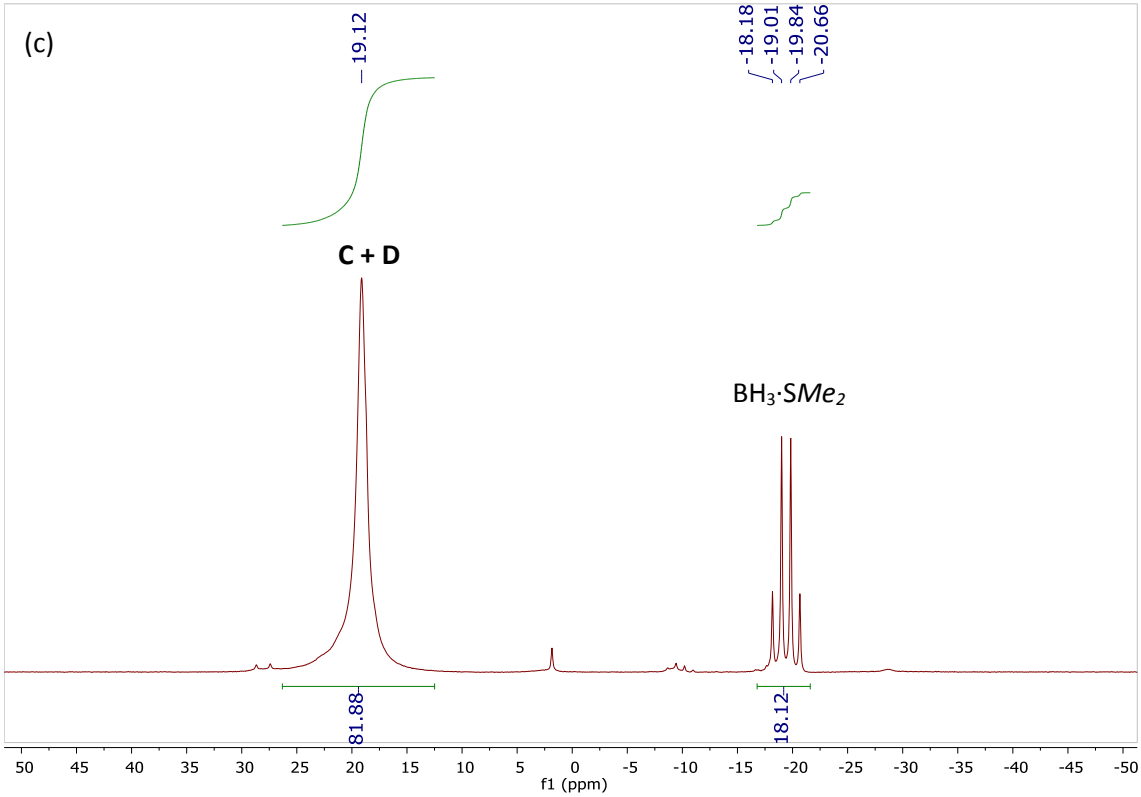
(c)
19.12
-18.18
-19.01
-19.84
-20.66
C + D
BH3·SMe2
81.88
18.12
f1 (ppm)

Fig S12. Total TON (●), and TON for the formation of $CH_2(OBC_8H_{14})_2$ (●) and $CH_3OBC_8H_{14}$ (●) *vs*. time (h) for the catalytic reduction of CO_2 with H-BC_8H_{14} at 60 ºC with DIC (a), compound **3** (b) and compound **4** (c) as catalysts (5 mol%).

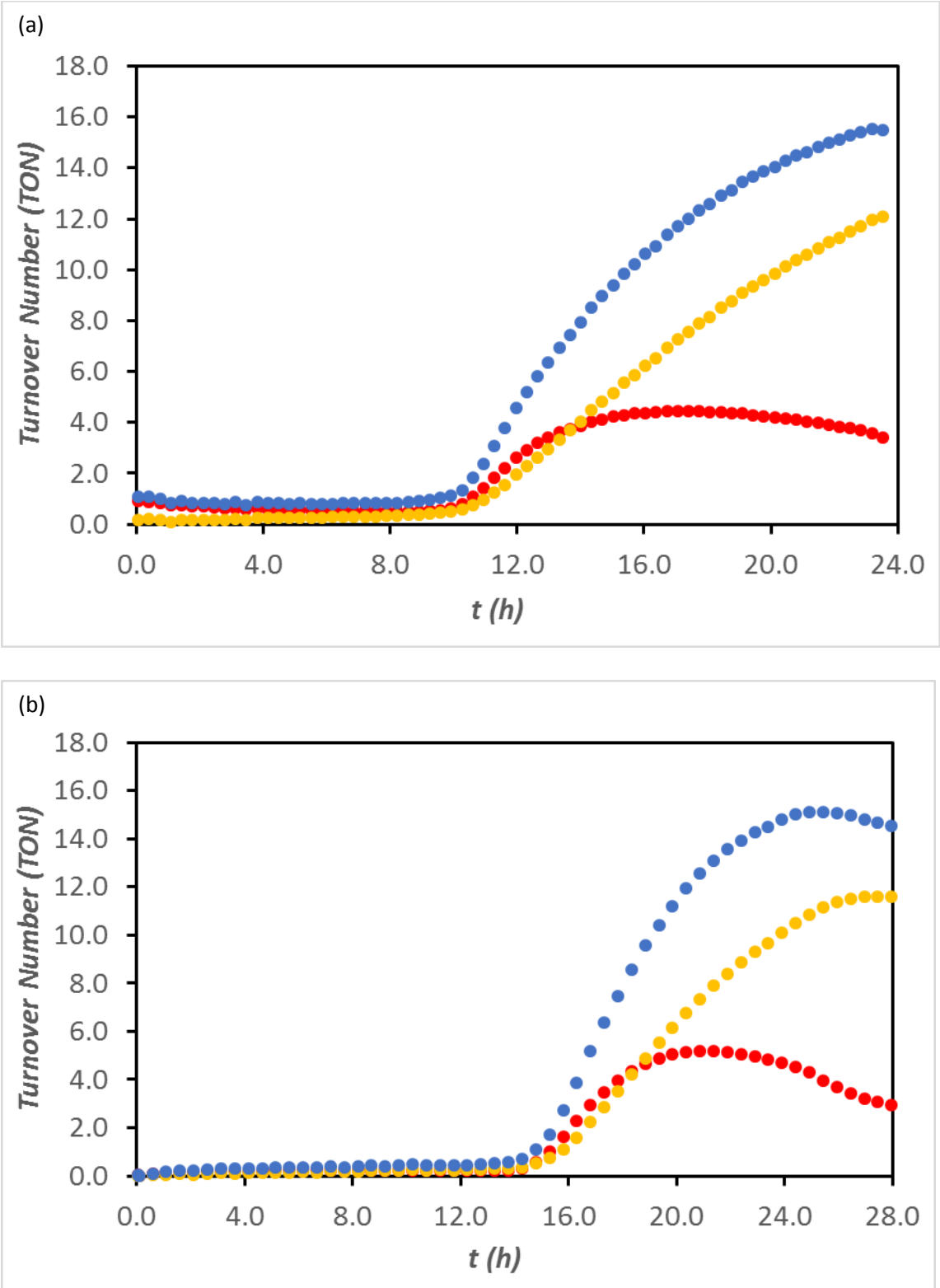

(c)

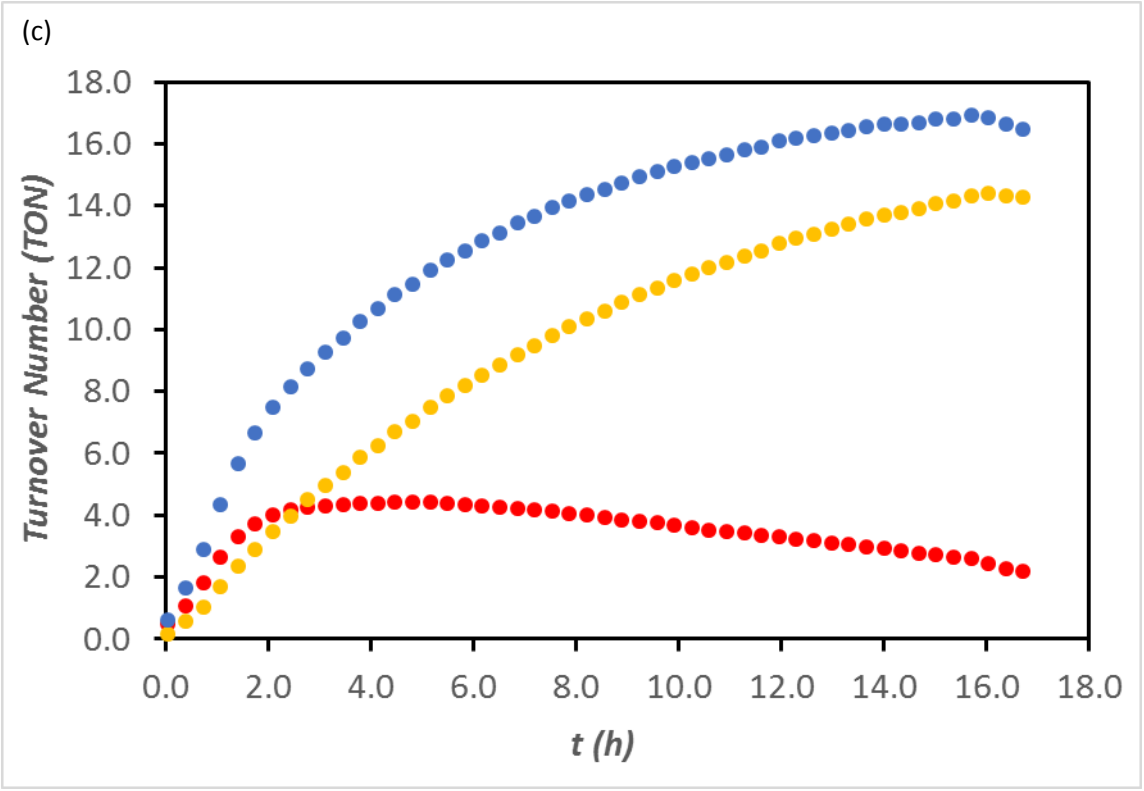
18.0
16.0
14.0
12.0
10.0
8.0
6.0
4.0
2.0
0.0
Turnover Number (TON)
0.0
2.0
4.0
6.0
8.0
10.0
12.0
14.0
16.0
18.0
t (h)

Fig S13. Distribution of products, $CH_2(OBC_8H_{14})_2$ (●) and $CH_3OBC_8H_{14}$ (●), and active species, compound **3** (●) and compound **4** (●), in mmol *vs*. time (h) for the catalytic reduction of CO_2 with H-BC_8H_{14} at 60 ºC with DIC (a), compound **3** (b) and compound **4** (c) as catalysts (5 mol%).

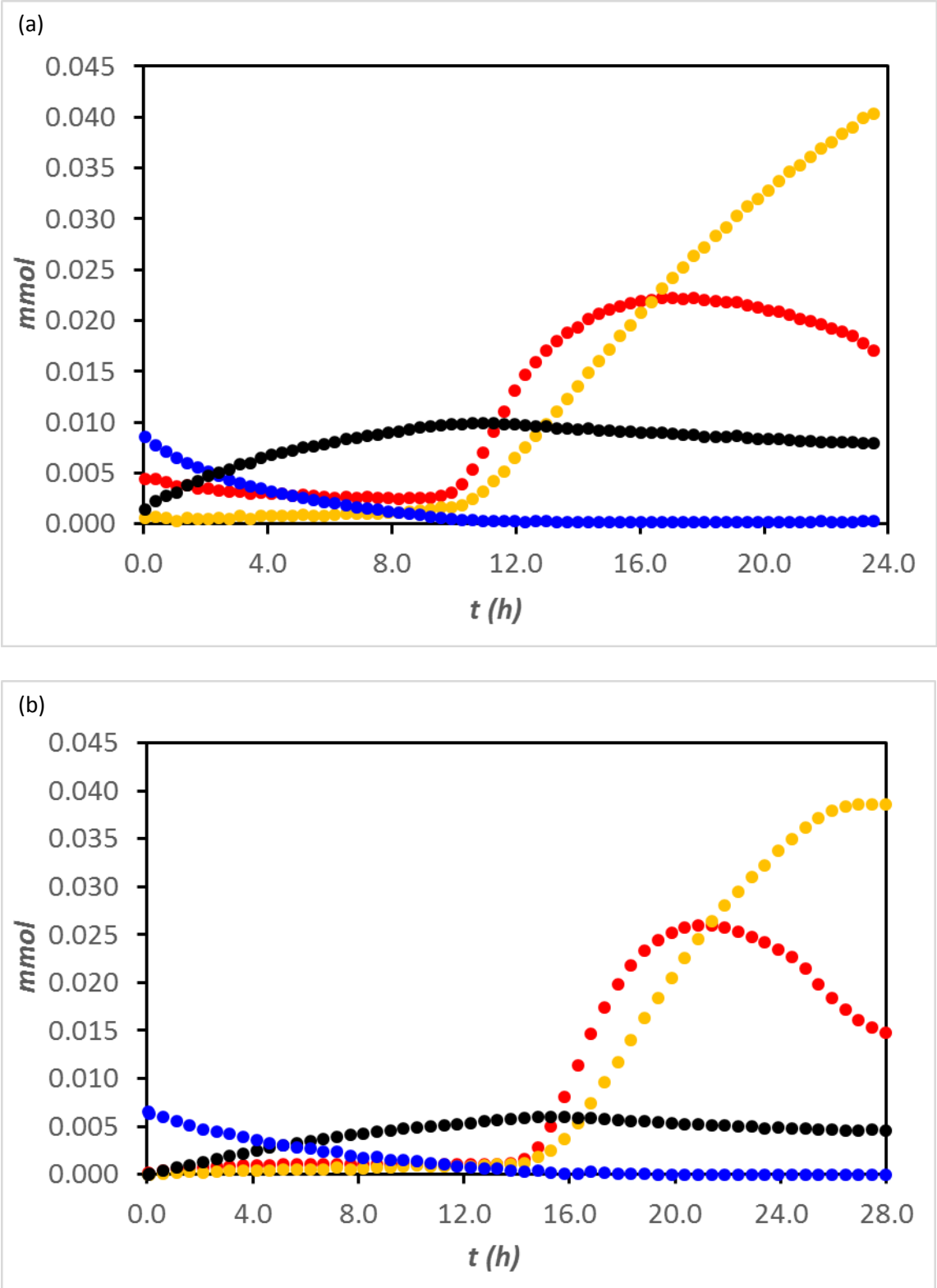

(c)

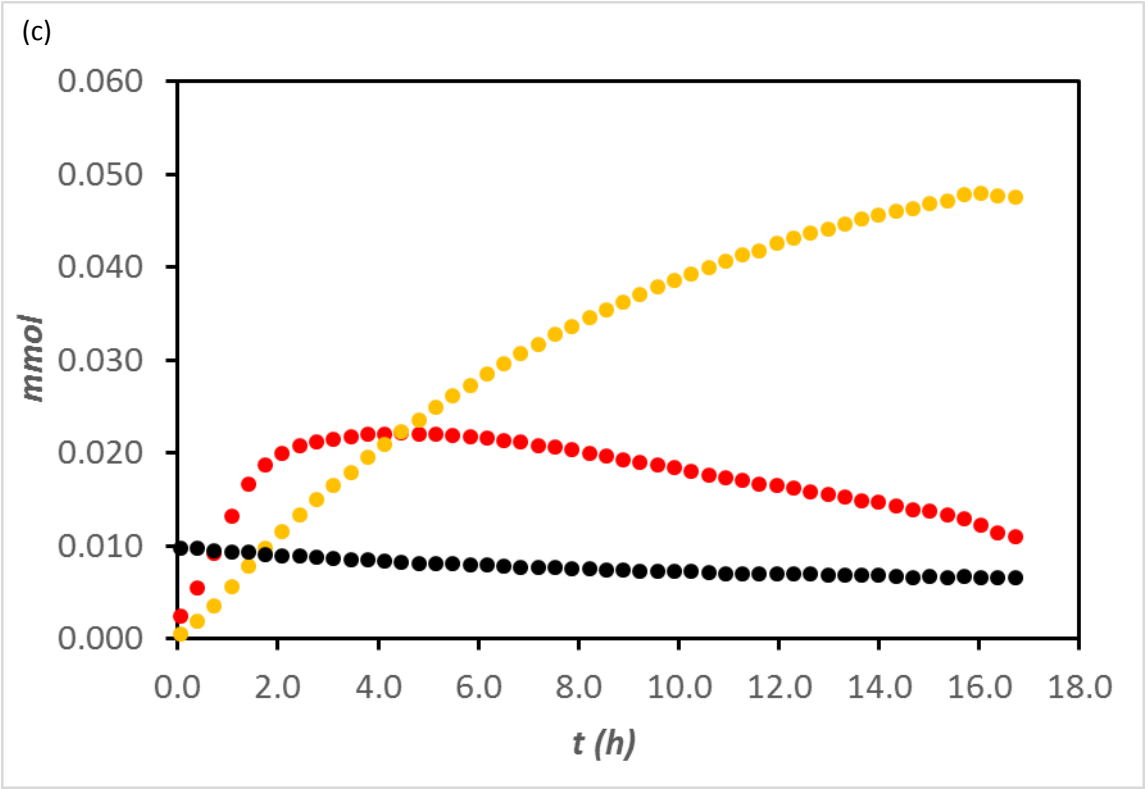
0.060
0.050
0.040
0.030
0.020
0.010
0.000
mmol
0.0
2.0
4.0
6.0
8.0
10.0
12.0
14.0
16.0
18.0
t (h)

X-ray crystal determination. X-ray data collection of suitable single crystals of compounds **2**, **3**, **4** and **5** were performed at 100(2) K on a Bruker VENTURE area detector equipped with graphite monochromated Mo-Kα radiation (λ = 0.71073 Å) by applying the ω-scan method. The data reduction was performed with the APEX2[4] software and corrected for absorption using SADABS.[5] Crystal structures were solved by direct methods using the SIR97 program[6] and refined by full-matrix least-squares on F^2 including all reflections using anisotropic displacement parameters by means of the WINGX crystallographic package.[7] All hydrogen atoms were included as fixed contributions riding on attached atoms with isotropic thermal displacement parameters 1.2 times or 1.5 times those of their parent atoms for the organic ligands except for those bound to boron atoms in compounds **2** and **5**, which were located. Details of the structure determination and refinement of compounds are summarised in Table S1. Crystallographic data (excluding structure factors) for the structures reported in this paper have been deposited with the Cambridge Crystallographic Data Centre as supplementary publication nos. CCDC 1829437-1829440. Copies of the data can be obtained free of charge on application to the Director, CCDC, 12 Union Road, Cambridge, CB2 1EZ, U.K. (Fax: +44-1223-335033; e-mail: deposit@ccdc.cam.ac.uk or http://www.ccdc.cam.ac.uk).

Fig S14. Molecular structures of compounds **2** (a), **3** (b) and **4** (c): C (grey), N (blue), O (red), B (pink). H atoms are omitted for clarity, except for the one bridging the B atoms in **2** (white). ORTEP ellipsoids are plotted at the 50% probability level.

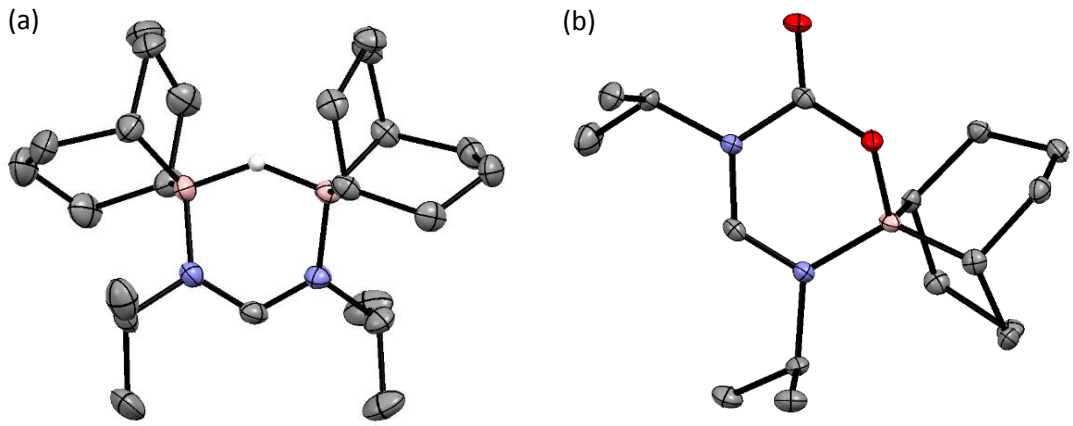

(c)

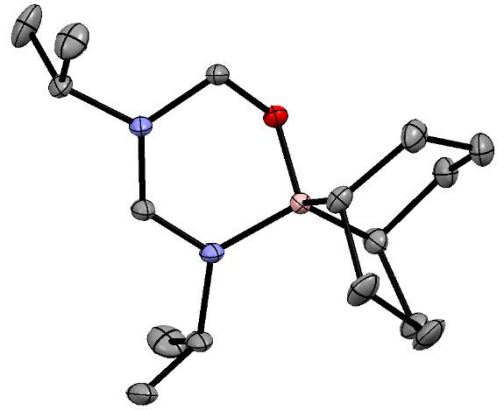

Table S1. Crystallographic data and structure refinement details for all compounds.

Compound	**2**	**3**	**4**	**5**
Chem. form.	$C_{23}H_{44}B_2N_2$	$C_{16}H_{29}BN_2O_2$	$C_{16}H_{31}BN_2O$	$C_{14}H_{34}B_2N_4$
CCDC	1829438	1829439	1829440	1829437
Form. weight	370.22	292.22	278.24	280.07
Cryst. system	Triclinic	Triclinic	Monoclinic	Orthorhombic
Space group	*P*-1	*P*-1	$P2_1/c$	$Pna2_1$
a (Å)	9.8852(7)	11.490(2)	11.8250(5)	20.751(3)
b (Å)	15.1771(9)	12.061(3)	18.6367(8)	14.369(3)
c (Å)	16.6307(12)	12.206(3)	19.5807(7)	5.598(2)
α (º)	69.154(2)	89.223(3)	90	90
β (º)	84.904(2)	86.315(3)	126.909(2)	90
γ (º)	79.674(3)	81.499(3)	90	90
V (Å^3)	2293.1(3)	1669.4(6)	3450.4(3)	1776.5(8)
Z	4	4	8	4
GOF [a]	1.049	1.040	1.057	1.055
R_{int}	0.1103	0.0964	0.1841	0.0448
R_1 [b] / wR^2 [c] [I>2σ(I)]	0.0654 / 0.1603	0.0541 / 0.1044	0.0513 / 0.1353	0.0396 / 0.0481
R_1 [b] / wR^2 [c] (all data)	0.1008 / 0.1855	0.0998 / 0.1208	0.0669 / 0.1456	0.0926 / 0.0973

[a] $S = [\sum w(F_0^2 - F_c^2)^2 / (N_{obs} - N_{param})]^{1/2}$ [b] $R_1 = \sum||F_0|-|F_c|| / \sum|F_0|$ [c] $wR_2 = [\sum w(F_0^2 - F_c^2)^2 / \sum wF_0^2]^{1/2}$

$w = 1/[\sigma^2(F_0^2) + (aP)^2 + bP]$ where $P = (\max(F_0^2,0) + 2Fc^2)/3$

Theoretical calculations. All the calculations were carried out by using the Gaussian09 suite of programs.[8] The M05–2X functional of Truhlar and co-workers[9] was employed to optimise all the equilibrium structures (catalysts, intermediates and transition states). This functional was parametrised for organic systems with non-covalent interactions and proved to be efficient and reliable for investigating reaction mechanisms. In particular, Cantat and co-workers have recently demonstrated the accuracy of this functional for the computation of reaction mechanisms for the metal-free reduction of CO_2 using highly related guanidines and amidines.[2a] A 6–31+G** basis set including polarisation and diffuse functions for heavy atoms and polarisation functions for the hydrogen atoms was used for all the computations.[10] Geometry optimisations were performed under no symmetry restrictions, and frequency analyses were performed for all the stationary points to ensure that minimum structures with no imaginary frequencies were achieved. Transition states were optimised through the Synchronous Transit-Guided Quasi-Newton (STQN) Method as implemented in Gaussian, characterised by frequency analysis (one imaginary frequency) and their connectivity was further corroborated through Intrinsic-Reaction-Coordinate (IRC) calculations. The free energies were calculated within the harmonic approximation for vibrational frequencies. Solvent effects (benzene, ε = 2.2706) were modelled using the polarised-continuum-model (PCM) of Tomasi and co-workers,[11] by using the gas-phase optimised structures.

Fig. S15 Computed reaction profile for the catalytic hydroboration of CO_2 with H-BBN and **4** as catalyst, Gibbs free energies in C_6H_6 expressed in kcal mol^{-1}.

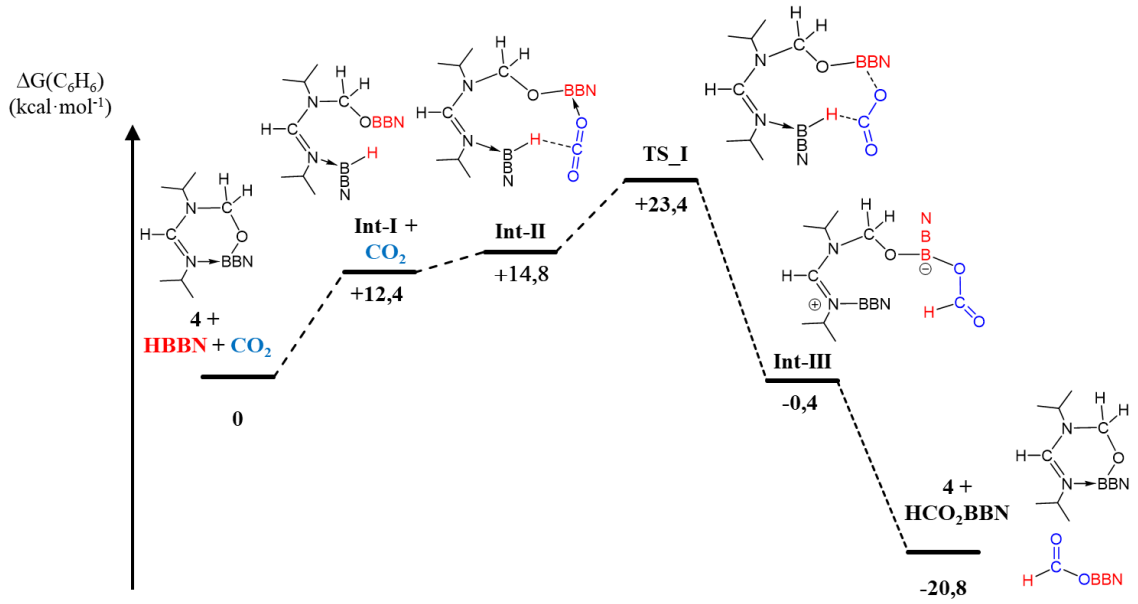

Table S2. Relative gas and solution (benzene) phase Gibbs free energies for the catalytic cycle of compound **4** (kcal·mol^{-1}).

	4 + H-BBN + CO_2	**Int-I** + CO_2	**Int-II**	**TS-I**	**Int-III**	**4** + HCO_2BBN
ΔG_{gas}	0	+11.7	+11.6	+21.9	-1.3	-18.4
$\Delta G_{C_6H_6}$	0	+12.4	+14.8	+23.4	-0.4	-20.8

Fig. S16 Computed reaction profile for the catalytic hydroboration of CO_2 with H-BBN and **1** as catalyst, Gibbs free energies in kcal mol^{-1}.

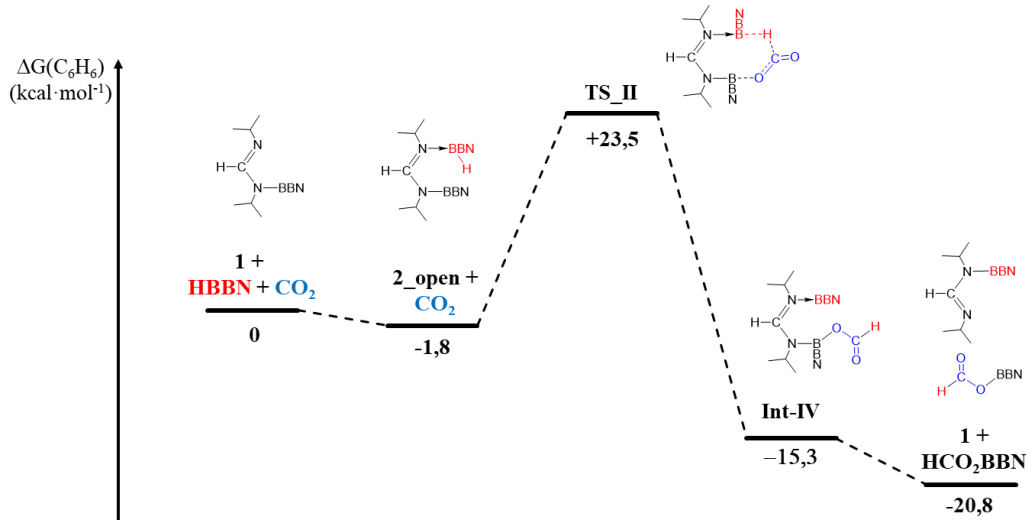

Table S3. Relative gas and solution (benzene) phase Gibbs free energies for the catalytic cycle of compound **1** (kcal·mol^{-1}).

	1 + H-BBN + CO_2	**2_open** + CO_2	**TS-II**	**Int-IV**	**1** + HCO_2BBN
ΔG_{gas}	0	-3.4	+21.8	-14.9	-18.4
$\Delta G_{C_6H_6}$	0	-1.8	+23.5	-15.3	-20.8

Fig. S17 Computed reaction profile for the catalytic hydroboration of CO_2 with $BH_3{\cdot}SMe_2$ and **5** as catalyst, Gibbs free energies in kcal mol^{-1}.

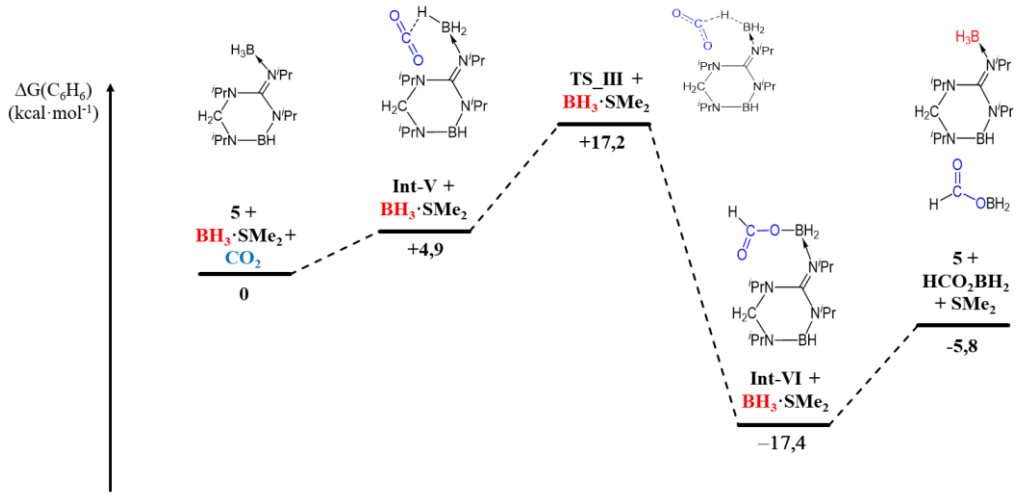

Table S4. Relative gas and solution (benzene) phase Gibbs free energies for the catalytic cycle of compound **5** (kcal·mol^{-1}).

	5 + $BH_3{\cdot}SMe_2$ + CO_2	**Int-V** + $BH_3{\cdot}SMe_2$	**TS-III** + $BH_3{\cdot}SMe_2$	**Int-VI** + $BH_3{\cdot}SMe_2$	**5** + HCO_2BH_2 + SMe_2
ΔG_{gas}	0	+3.8	+18.7	-18.9	-5.7
$\Delta G_{C_6H_6}$	0	+4.9	+17.2	-17.3	-5.8

Table S5. Relative gas phase Gibbs free energies for the non-catalysed first hydroboration of CO_2 with $BH_3{\cdot}SMe_2$ and H-BBN (kcal·mol^{-1}).[a]

	$BH_3{\cdot}SMe_2$ + CO_2	H-BBN + CO_2
ΔG_{gas}	+32.1	+29.6

[a] Energies corresponding to the transition states for the hydride migration from B to C, and referenced to the isolated reactants.

REFERENCES

1. (a) T. Wang and D. W. Stephan, *Chem. Commun.*, 2014, **50**, 7007-7010; (b) Y. Yang, M. Xu and D. Song, *Chem. Commun.*, 2015, **51**, 11293-11296.
2. (a) C. Das Neves Gomes, E. Blondiaux, P. Thuéry and T. Cantat, *Chem. Eur. J.*, 2014, **20**, 7098-7106; (b) S. C. Sau, R. Bhattacharjee, P. K. Vardhanapu, G. Vijaykumar, A. Datta and S. K. Mandal, *Angew. Chem. Int. Ed.*, 2016, **55**, 15147-15151.
3. (a) G. Povie, G. Villa, L. Ford, D. Pozzi, C. H. Schiesser and P. Renaud, *Chem. Commun.*, 2010, **46**, 803-805; (b) S. Y. F. Ho, C.-W. So, N. Saffon-Merceron and N. Mézailles, *Chem. Commun.*, 2015, **51**, 2107-2110; (c) M.-A. Courtemanche, M.-A. Légaré, L. Maron and F.-G. Fontaine, *J. Am. Chem. Soc.*, 2013, **135**, 9326-9329; (d) K. Fujiwara, S. Yasuda and T. Mizuta, *Organometallics*, 2014, **33**, 6692-6695.
4. Bruker Apex2, Bruker AXS Inc., Madison, Wisconsin, USA, 2004.
5. G. M. Sheldrick, SADABS, Program for Empirical Adsorption Correction, Institute for Inorganic Chemistry, University of Gottingen: Germany, 1996.
6. A. Altomare, M. C. Burla, M. Camalli, G. L. Cascarano, C. Giacovazzo, A. Guagliardi, A. G. G. Moliterni, G. Polidori and R. Spagna, *J. Appl. Crystallogr.*, 1999, **32**, 115-119.
7. (a) G. M. Sheldrick, SHELX-2014, Program for Crystal Structure Refinement, University of Göttingen, Göttingen, Germany, 2014; (b) L. Farrugia, *J. Appl. Crystallogr.*, 1999, **32**, 837-838.
8. M. J. Frisch, G. W. Trucks, H. B. Schlegel, G. E. Scuseria, M. A. Robb, J. R. Cheeseman, G. Scalmani, V. Barone, B. Mennucci, G. A. Petersson, H. Nakatsuji, M. Caricato, X. Li, H. P. Hratchian, A. F. Izmaylov, J. Bloino, G. Zheng, J. L. Sonnenberg, M. Hada, M. Ehara, K. Toyota, R. Fukuda, J. Hasegawa, M. Ishida, T. Nakajima, Y. Honda, O. Kitao, H. Nakai, T. Vreven, J. A. Montgomery, J. E. Peralta, F. Ogliaro, M. Bearpark, J. J. Heyd, E. Brothers, K. N. Kudin, V. N. Staroverov, R. Kobayashi, J. Normand, K. Raghavachari, A. Rendell, J. C. Burant, S. S. Iyengar, J. Tomasi, M. Cossi, N. Rega, J. M. Millam, M. Klene, J. E. Knox, J. B. Cross, V. Bakken, C. Adamo, J. Jaramillo, R. Gomperts, R. E. Stratmann, O. Yazyev, A. J. Austin, R. Cammi, C. Pomelli, J. W. Ochterski, R. L. Martin, K. Morokuma, V. G. Zakrzewski, G. A. Voth, P. Salvador, J. J. Dannenberg, S. Dapprich, A. D. Daniels, Farkas, J. B. Foresman, J. V. Ortiz, J. Cioslowski and D. J. Fox, 2009, DOI: citeulike-article-id:9096580.
9. Y. Zhao, N. E. Schultz and D. G. Truhlar, *J. Chem. Theory Comput.*, 2006, **2**, 364-382.
10. (a) G. A. Petersson and M. A. Al-Laham, *J. Chem. Phys.*, 1991, **94**, 6081-6090; (b) G. A. Petersson, A. Bennett, T. G. Tensfeldt, M. A. Al-Laham, W. A. Shirley and J. Mantzaris, *J. Chem. Phys.*, 1988, **89**, 2193-2218.
11. (a) J. Tomasi, B. Mennucci and R. Cammi, *Chem. Rev.*, 2005, **105**, 2999-3094; (b) M. Cossi, V. Barone, R. Cammi and J. Tomasi, *Chem. Phys. Lett.*, 1996, **255**, 327-335.